Downloaded from genome.cshlp.org on June 13, 2026 . Published by Cold Spring Harbor Laboratory Press

Distinct types of short open reading frames are translated in plant cells

Igor Fesenko, Ilya Kirov, Andrey Knyazev, et al.

Genome Res. published online August 6, 2019
Access the most recent version at doi:10.1101/gr.253302.119

P<P Published online August 6, 2019 in advance of the print journal.

Accepted Manuscript Peer-reviewed and accepted for publication but not copyedited or typeset; accepted manuscript is likely to differ from the final, published version.

Creative Commons License This article is distributed exclusively by Cold Spring Harbor Laboratory Press for the first six months after the full-issue publication date (see http://genome.cshlp.org/site/misc/terms.xhtml). After six months, it is available under a Creative Commons License (Attribution-NonCommercial 4.0 International), as described at http://creativecommons.org/licenses/by-nc/4.0/.

Email Alerting Service Receive free email alerts when new articles cite this article - sign up in the box at the top right corner of the article or **click here.**

Advance online articles have been peer reviewed and accepted for publication but have not yet appeared in the paper journal (edited, typeset versions may be posted when available prior to final publication). Advance online articles are citable and establish publication priority; they are indexed by PubMed from initial publication. Citations to Advance online articles must include the digital object identifier (DOIs) and date of initial publication.

To subscribe to *Genome Research* go to:
https://genome.cshlp.org/subscriptions

Published by Cold Spring Harbor Laboratory Press

Downloaded from genome.cshlp.org on June 13, 2026 . Published by Cold Spring Harbor Laboratory Press

Distinct types of short open reading frames are translated in plant cells

Igor Fesenko[1,*], Ilya Kirov[2], Andrey Kniazev[1], Regina Khazigaleeva[1], Vassili Lazarev[3,4], Daria Kharlampieva[3], Ekaterina Grafskaia[3,4], Viktor Zgoda[5], Ivan Butenko[3], Georgy Arapidi[1,3], Anna Mamaeva[1], Vadim Ivanov[1], Vadim Govorun[3].

[1]Laboratory of functional genomics and plant proteomics, Shemyakin and Ovchinnikov Institute of Bioorganic Chemistry, Moscow, Russian Federation; [2]Laboratory of marker-assisted and genomic selection of plants, All-Russian Research Institute of Agricultural Biotechnology, Moscow, Russian Federation; [3] Research Institute for Physico-Chemical Medicine, Moscow, Russian Federation; [4]Moscow Institute of Physics and Technology, Dolgoprudny, Moscow region, Russia; [5]Laboratory of System Biology, Institute of Biomedical Chemistry, Moscow, Russian Federation.

Corresponding author(s).

***** Igor Fesenko, e-mail: fesigor@gmail.com

Running title: Translation of sORFs in moss

Keywords: short open reading frames, plant peptides, LC-MS/MS, evolution, alternative splicing, lncRNA

ABSTRACT

Genomes contain millions of short (<100 codons) open reading frames (sORFs), which are usually dismissed during gene annotation. Nevertheless, peptides encoded by such sORFs can play important biological roles, and their impact on cellular processes has long been underestimated. Here, we

Downloaded from genome.cshlp.org on June 13, 2026 . Published by Cold Spring Harbor Laboratory Press

analyzed approximately 70,000 transcribed sORFs in the model plant *Physcomitrella patens* (moss). Several distinct classes of sORFs that differ in terms of their position on transcripts and the level of evolutionary conservation are present in the moss genome. Over 5000 sORFs were conserved in at least one of ten plant species examined. Mass spectrometry analysis of proteomic and peptidomic datasets suggested that tens sORFs located on distinct parts of mRNAs and long non-coding RNAs (lncRNAs) are translated, including conserved sORFs. Translational analysis of the sORFs and main ORFs at a single locus suggested the existence of genes that code for multiple proteins and peptides with tissue-specific expression. Functional analysis of four lncRNA-encoded peptides showed that sORFs-encoded peptides are involved in regulation of growth and differentiation in moss. Knocking out lncRNA-encoded peptides resulted in a decrease of moss growth. By contrast, the overexpression of these peptides resulted in a diverse range of phenotypic effects. Our results thus open new avenues for discovering novel, biologically active peptides in the plant kingdom.

INTRODUCTION

The genomes of nearly all organisms contain hundreds of thousands of short open reading frames (sORFs; <100 codons) whose coding potential has been the subject of recent reviews (Andrews and Rothnagel 2014; Couso 2015; Hellens et al. 2016; Couso and Patraquim 2017; Rothnagel and Menschaert 2018; Ruiz-Orera and Alba 2019). However, gene annotation algorithms are generally not suited for dealing with sORFs because short sequences are unable to obtain high conservation scores, which serve as an indicator of functionality (Ladoukakis et al. 2011). Nevertheless, using various bioinformatic approaches, sORFs with high coding potential have been identified in a range of organisms including fruit flies, mice, yeast and *Arabidopsis thaliana* (Ladoukakis et al. 2011; Hanada et al. 2013; Aspden et al. 2014; Bazzini et al. 2014). The first systematic study of sORFs was conducted on baker's yeast, where 299 previously non-annotated sORFs were identified and tested in genetic experiments (Kastenmayer et al. 2006). Subsequently, 4561 conserved sORFs were identified in the genus *Drosophila*, 401 of which were postulated to be

Downloaded from genome.cshlp.org on June 13, 2026 . Published by Cold Spring Harbor Laboratory Press

functional, taking into account their syntenic positions, low K_A/K_S (<0.1) values and transcriptional evidence (Ladoukakis et al. 2011). In a recent study, Mackowiak and colleagues predicted the presence of 2002 novel conserved sORFs (from 9 to 101 codons) in *Homo sapiens*, *Mus musculus*, *Danio rerio*, *Drosophila melanogaster* and *Caenorhabditis elegans* (Mackowiak et al. 2015). The first comprehensive study of sORFs in plants postulated the existence of thousands of sORFs with high coding potential in *Arabidopsis* (Lease and Walker 2006; Hanada et al. 2007; Hanada et al. 2013), including 49 that induced various morphological changes and had visible phenotypic effects.

Recent studies have pointed to the important roles of sORF-encoded peptides (SEPs) in cells (Magny et al. 2013; Nelson et al. 2016; D'Lima et al. 2017; Huang et al. 2017; Matsumoto et al. 2017; Rubtsova et al. 2018). However, unraveling the roles of SEPs is a challenging task, as is their detection at the biochemical level. In animals, SEPs are known play important roles in a diverse range of cellular processes (Kondo et al. 2010; Magny et al. 2013). By contrast, only a few functional SEPs have been reported in plants, including POLARIS (PLS; 36 amino acids), EARLY NODULIN GENE 40 (ENOD40; 12, 13, 24 or 27 amino acids), ROTUNDIFOLIA FOUR (ROT4; 53 amino acids), KISS OF DEATH (KOD; 25 amino acids), BRICK1 (BRK1; 84 amino acids), Zm-908p11 (97 amino acids) and Zm-401p10 (89 amino acids) (Andrews and Rothnagel 2014; Tavormina et al. 2015). These SEPs help modulate root growth and leaf vascular patterning (Chilley et al. 2006), symbiotic nodule development (Djordjevic et al. 2015), polar cell proliferation in lateral organs and leaf morphogenesis (Narita et al. 2004), and programmed cell death (apoptosis) (Blanvillain et al. 2011).

To date, functional sORFs have been found in a variety of transcripts, including untranslated regions of mRNA (5′ leader and 3′ trailer sequences), lncRNAs, and microRNA transcripts (pri-miRNAs) (Andrews and Rothnagel 2014; Laing et al. 2015; Lauressergues et al. 2015; Couso and Patraquim 2017; Brunet et al. 2019). Evidence for the transcription of potentially functional sORFs has been obtained in *Populus deltoides*, *Phaseolus vulgaris*, *Medicago truncatula*, *Glycine max* and *Lotus japonicus* (Guillen et al. 2013). The transcription of sORFs can be regulated by stress conditions and depends on the developmental stage of the plant (De Coninck et al. 2013; Hanada et al. 2013; Rasheed et al. 2016). Indeed, sORFs might represent an important source of advanced traits required under stress conditions. During stress, genomes undergo widespread

Downloaded from genome.cshlp.org on June 13, 2026 . Published by Cold Spring Harbor Laboratory Press

transcription to produce a diverse range of RNAs (Kim et al. 2010; Mazin et al. 2014); therefore, a large portion of sORFs becomes accessible to the translation machine for peptide production. Stress conditions can lead to the transcription of sORFs located in genomic regions that are usually non-coding (Giannakakis et al. 2015). Such sORFs appear to serve as raw materials for the birth and subsequent evolution of new protein-coding genes (Couso and Patraquim 2017; Ruiz-Orera and Alba 2019).

The transcription of an sORF does not necessarily indicate that it fulfills any biological role, as opposed to being a component of the so-called translational noise (Guttman et al. 2013). According to ribosomal profiling data, thousands of lncRNAs display high ribosomal occupancy in regions containing sORFs in mammals (Ingolia et al. 2011; Aspden et al. 2014; Bazzini et al. 2014). However, lncRNAs can have the same ribosome profiling patterns as canonical non-coding RNAs (e.g., rRNA) that are known not to be translated, implying that these lncRNAs are unlikely to produce functional peptides (Guttman et al. 2013). In addition, identification of SEPs via mass spectrometry analyses has found many fewer peptides than predicted sORFs (Slavoff et al. 2013; Aspden et al. 2014). Thus, the abundance, lifetime and other features of SEPs are generally unclear.

We performed a comprehensive analysis of the sORFs that have canonical AUG start codons and high coding potential in the *Physcomitrella patens* genome. The translation of tens of sORFs was confirmed by mass-spectrometry analysis. From these, candidate lncRNA-encoded peptides were selected for further analysis, which provided evidence for their biological functions.

RESULTS

Discovery and classification of potential coding sORFs in the moss genome

Our approach is summarized in Fig. 1A. At the first stage of analysis, we used the sORF finder tool (Hanada et al. 2010) to identify single-exon sORFs starting with an AUG start codon and less than 300 bp long. This approach resulted in the identification of 638,439 sORFs with coding potential (CI index) in all regions of the *P. patens* genome.

We selected 70,095 unique sORFs located on transcripts annotated in the moss genome (phytozome.jgi.doe.gov) and/or our dataset (Fesenko et al. 2015) for further analysis, as well as

Downloaded from genome.cshlp.org on June 13, 2026 . Published by Cold Spring Harbor Laboratory Press

those on lncRNAs from two databases - CANTATAdb (Szczesniak et al. 2016) and GreeNC (Paytuvi Gallart et al. 2016); sORFs located in repetitive regions were discarded (Supplemental Table S1). These selected sORFs, which were 33 to 303 bp long, were located on 33,981 transcripts (22,969 genes), with up to 28 sORFs per transcript (Supplemental Fig. S1A).

We then classified the sORFs based on their location on the transcript: 63,109 "genic-sORFs" (located on annotated transcripts, but not on lncRNA), 1241 "intergenic-sORFs" (located on transcripts from our dataset and not annotated in the current version of the genome) and 5745 "lncRNA-sORFs" (located on lncRNAs from CANTATAdb (Szczesniak et al. 2016), GreeNC (Paytuvi Gallart et al. 2016) or our data set (Fesenko et al. 2017); Fig. 1B). The genic-sORFs include 11,998 upstream ORFs (uORFs; for 5'-UTR location), 9443 downstream ORFs (dORFs; for 3'-UTR location), 36,732 coding sequence-sORFs (CDS-sORFs; sORFs overlapping with main ORFs (+1 frame) in non-canonical +2 and +3 reading frames) and 3485 interlaced-sORFs (overlapping with both the CDS and 5'-UTR or CDS and 3'-UTR on the same transcript) (Fig. 1B, Supplemental Fig. S1B).

As expected based on the sORF finder search strategy (Hanada et al. 2010), the sORF set was enriched in CDS-sORFs (52%, Fisher's exact test, *P*-value < 10^{-16}), whereas dORFs, uORFs and interlaced-sORFs were underrepresented (Fisher's exact test, *P*-value < 10^{-16}) compared to a random exonic fragments set, which was used as a negative control. On average, CDS-sORFs (median size of 22 codons) were shorter than uORFs (median size of 35 codons; Mann-Whitney *U* test *P*-value < 10^{-16}) and dORFs (median length 32 codons, Mann-Whitney *U* test *P*-value < 10^{-16}). The median size of interlaced-sORFs was 49 codons, which is significantly longer than other genic-sORFs (Mann-Whitney *U* test P = 0.0021) (Fig. 1C).

To estimate the number of conserved transcriptable sORFs, we performed a TBLASTN search (e-value cutoff 0.00001) of each sORF sequence against the reconstructed genomes of three *P. patens* ecotypes, Villersexel, Reute, and Kaskasia, as well as the transcriptomes of ten plant species (Supplemental Fig. S2). We found 5034 conserved sORFs with detectable homologous sequences in at least one species (Supplemental Table S1, Supplemental Fig. S3). A conservation analysis of the sORFs in the reconstructed *P. patens* ecotypes showed that 2.4% (1618) of the sORFs were lacking either the start or stop codons in at least one species. We then examined the differences in selection

Downloaded from genome.cshlp.org on June 13, 2026 . Published by Cold Spring Harbor Laboratory Press

pressure at the amino acid level between different major groups of conservative sORFs (CDS-sORFs, uORFs, dORFs, lncRNA-sORFs, interlaced-sORFs) using the criterion of K_A/K_S. Higher retention rates were observed for uORFs and dORFs, whereas CDS-sORFs and lncRNA-ORFs were under strong positive selection (Supplemental Fig. S4). These observations are in agreement with the fact that some type of sORFs (for example, uORFs) play a regulatory role instead of being translated (Barbosa et al. 2013).

Experimental evidence for the translation of sORFs

Obtaining evidence for the translation of sORFs is an important step towards identifying functional SEPs. We analyzed the Kozak consensus sequences (Kozak 1986) surrounding sORF start codons. Kozak consensus sequence plays an important role in translation initiation (Kozak 1997). Depending on the presence of the purine in position −3 and the G in position +4 (where +1 is "A" in the "AUG" codon) the Kozak was considered to be "strong" (both are present), "medium" (one is present) or "weak" (neither are present) (Kozak 1997). According to our results, 41816 (~60%) of the predicted sORFs were surrounded by "strong" and "medium" Kozak sequences. These values were significantly smaller than those of annotated protein coding ORFs (87%, Fisher's exact test *P*-value < 2.2×10^{-16}).

We then verified the translation of our predicted sORFs using mass-spectrometry (MS) analysis. Taking into account the shortage of proteomic methods for identifying small proteins or peptides, in the current study, we generated two datasets: the "peptidomic" dataset - endogenous peptides extracted from three types of moss cells: gametophores, protonemata and protoplasts and the "proteomic" dataset - tryptic peptides generated in a standard proteomic pipeline (Supplemental Table S2). All datasets were mapped with MaxQuant against a custom database containing our sORFs together with nuclear, chloroplast and mitochondrial moss protein sequences (see details in the Methods). PSMs (peptide spectrum matches) were identified at 1% FDR, and ambiguous peptides were filtered out. This resulted in 1177 PSMs corresponding to 296 distinct peptide sequences in the peptidomic dataset and 920 PSMs corresponding to 532 peptide sequences in the proteomic dataset. To generate a high-confidence sORF candidate set, we increased our acceptance threshold to a minimum Posterior Error Probability (PEP) of 0.01 and Andromeda score of higher than 60. The final

Downloaded from genome.cshlp.org on June 13, 2026 . Published by Cold Spring Harbor Laboratory Press

set underwent a manual inspection of spectra. As a result, we confirmed the translation of 46 sORFs: 17 in gametophores, 29 in protonemata, and 14 in protoplasts ("confident sORFs", Fig. 2A, Supplemental Table S3). The length of these small protein-coding sORFs ranged from 14 to 99 amino acids (aa), which were generally longer than untranslatable sORFs (Mann-Whitney *U* test *P*-value = 5.33×10^{-6}) (Fig. 2B). We observed that PSMs supporting SEP identifications had lower average quality than those mapped to the protein sequences (Supplemental Figs. S5A and S5B). This finding is in agreement with data obtained for the animal kingdom (Slavoff et al. 2013; Mackowiak et al. 2015). The quality of spectra and the values of PSMs supporting the expression of SEPs were better in the "peptidomic" dataset (Supplemental Fig. S5C). Also, translatable sORFs were longer for those identified in the peptidomic dataset (Supplemental Fig. S5D). Approximately 63% of the translated sORFs (29 sORFs) contained "strong" and "medium" Kozak elements, which is similar to the results obtained for all predicted sORFs (~60%). This result suggests that translation initiation may differ for sORFs and protein coding ORFs.

The most prominent group of small protein-coding sORFs consisted of CDS-sORFs (19 sORFs, 41.3%) (Fig. 2C). Also, the translation of uORFs (6 sORFs, 13%) and dORFs (9 sORFs, 19.6%) was confirmed by our analysis. Based on our MS data, we identified seven loci with at least two translated ORFs (annotated as main ORF and sORF), including 5 CDS-sORFs, that represent putative multi-coding genes (Fig. 2D; Supplemental Table S4). Some of the putative multi-coding genes were translated simultaneously with protein-coding ORFs in the same type of moss cell (e.g. Pp3c11_sORF461), while others showed different patterns of sORF and main ORF translation (e.g. Pp3c1_sORF1909). These findings indicate that small protein-coding CDS-sORFs are expressed simultaneously with main ORFs and the translation of sORFs and proteins located together in the same locus might be regulated in a tissue-specific manner.

The translation of 9 sORFs located on lncRNAs was also detected by our analysis. The level of transcription of some lncRNAs (according to the previous data (Fesenko et al. 2017) and Phytozome 12.0 expression atlas) and evidences of translation for the corresponding lncRNA-sORFs are shown in Fig. 2E. Three of these SEPs, Pp3c18_sORF57 (40aa), Pp3c9_sORF1544 (41aa) and Pp3c25_sORF1000 (61aa), were common to all three cell types and were confirmed by several

Downloaded from genome.cshlp.org on June 13, 2026 . Published by Cold Spring Harbor Laboratory Press

unique endogenous peptides (Fig. 2E). These data may point to biological significance for the peptides translated from these sORFs rather than the sORFs having regulatory functions in the translation of the main ORF. To explore this notion, we investigated the functions of four SEPs encoded by lncRNAs (see below).

Most small protein-coding sORFs are not evolutionarily conserved

Analysis of the evolutionary conservation of sORFs is often a key step in revealing biologically active sORFs (Andrews and Rothnagel 2014). To investigate whether the trend in small protein-coding sORF evolution differs from that of the other sORFs, we estimated the number of species in which homologs can be found and the selection pressure (K_A/K_S) on translatable sORFs on an evolutionary timescale using the transcriptomes of the ten abovementioned species. Overall, we found 5 sORFs had evidence of translation and conservation in at least one species, 4 of them were under negative selection ($K_A/K_S << 1$). Thus, analysis of sORF sequence conservation showed that only 11% of our small protein-coding sORFs have signature of conservation between species.

Alternative splicing regulates the number of sORFs in protein-coding transcripts

Alternative splicing (AS) is a universal process among eukaryotic organisms and more than 50% of *P. patens* genes are alternatively spliced (Chang et al. 2014; Wu et al. 2014; Fesenko et al. 2017). AS events may lead to the specific gain, loss or truncation of different groups of sORFs located on the transcripts of the same gene. We found 6092 alternatively spliced sORFs (AS-sORFs) belonging to transcripts from 4389 genes. CDS-sORFs were significantly overrepresented (Supplemental Fig. S6) while interlaced-sORFs, uORFs and dORFs were significantly underrepresented among AS-sORFs compared to the control set of random exonic fragments. We found that about half of the entire set of AS-sORFs (48%, 2933) underwent complete excision (complete sORF removal from an isoform; Fig. 3). The complete excision of sORFs occurred significantly more frequently in uORFs (57% of all AS-sORFs) than in the other AS-sORF groups (20–44% of all AS-sORFs, Fisher's exact test *P*-value $< 10^{-6}$). Among small protein-coding AS-sORFs, we found 3 affected by stop codon excision. 2 of the

Downloaded from genome.cshlp.org on June 13, 2026 . Published by Cold Spring Harbor Laboratory Press

translatable AS-sORFs were affected by start codon excision and one undergone complete excision. We then randomly selected thirteen different AS-sORFs with/without evidence of translation and searched for the corresponding isoforms in the transcriptomes of three types of moss cells. RT-PCR analysis revealed the transcription of these isoforms, confirming that they could indeed be translated (Supplemental Fig. S7). Moreover, some sORFs contained isoforms showing tissue-specific transcription. These observations led to the hypothesis that the translation of sORFs is regulated by AS.

The formation of a premature termination codon (PTC) as a result of alternative splicing events, might lead to mRNA decay (Ge and Porse 2014; Karousis et al. 2016) and rapid nonsense-mediated decay (NMD)-coupled degradation of sORF-encoded peptides (Popp and Maquat 2013). Using recently published transcriptomic data from moss NMD-deficient mutants (Lloyd et al. 2018), we investigated whether our translatable sORFs were present on NMD-targeted transcripts. The only one CDS-sORF (Pp3c7_sORF1583) was potentially present on such transcripts. Therefore, it is difficult to judge if AS-sORFs can trigger NMD-dependent transcript degradation.

Thus, our analysis demonstrated that AS might regulates the excision of sORFs from the transcriptome of *P. patens*, preventing AS-sORF translation by start or stop codon as well as complete sORF excision.

The sequence similarity analysis reveals sORFs with high identity to coding genes

Competitive inhibitors of protein–protein interactions (PPI) are referred to as MicroProteins (miPs) or small interfering peptides (siPEPs) and can be generated by alternative splicing or evolutionarily generated by domain loss (Seo et al. 2011; Staudt and Wenkel 2011; Eguen et al. 2015). Using BLASTP (e-value < 10^{-6}) similarity searches, we identified 363 sORFs resulting from AS events that partially overlapped with the main ORF, thereby generating truncated versions of the proteins (cis-sORFs; Supplemental Table S5). We found that 60 cis-sORFs harbored intrinsically disordered regions (IDRs, (van der Lee et al. 2014)), while 30 ones contained parts of 28 different domains (Supplemental Table S5). However, we did not identify small protein-coding cis-sORFs in our dataset.

Downloaded from genome.cshlp.org on June 13, 2026 . Published by Cold Spring Harbor Laboratory Press

It could be explained by a significant overlap with the protein sequences, whereas we filtered out the 'ambiguous' PSMs.

We then identified 272 sORFs that shared similarity with annotated proteins but were located on other transcripts (trans-sORFs, see in Supplemental Table S5). Trans-sORFs may have originated through the divergence of ancient paralogous genes, which occurred after the paleo duplication of the moss genome (Rensing et al. 2007; Rensing et al. 2008). In fact, 159 (58.5%) trans-sORFs shared similarity to genes from at least one species. In addition, all of these trans-sORFs are under strong purifying selection ($K_A/K_S << 1$).

Several distinct clusters with sORF-encoded peptides sharing similarity with more than four proteins from distinct genes were detected (Supplemental Fig. S8). Each cluster encompasses genes from different protein families, including one containing leucine-rich repeat and zinc-finger domains involved in protein–protein and protein–nucleic acid interactions, respectively. We examined the co-expression data and compared the distribution of correlation coefficient values between potential SEPs and their targets with those from randomly selected pairs (10 iterations) of genes. On average, these sORF-protein pairs had higher correlation coefficients than randomly selected gene pairs (Wilcoxon Rank Sum and Kolmogorov-Smirnov Tests P-value < 0.05), implying that sORF-bearing and target genes are frequently co-expressed.

SEPs regulate moss growth

Despite the recent finding that 10% of overexpressed intergenic sORFs have clear phenotypes in *Arabidopsis* (Hanada et al. 2013), the functions of most sORFs and SEPs in plants are generally unknown. Known bioactive SEPs in plants are encoded by sORFs located on short non-protein-coding transcripts, which can be referred to as lncRNAs (Rohrig et al. 2002; Chilley et al. 2006). In this context, it would be importantly to determine how many plant lncRNAs encode peptides, as well as the biological functions of these SEPs. Our pipeline allowed us to identify translated sORFs, including those encoded by lncRNAs. Some of these lncRNA-sORFs showed tissue-specific transcription and translation patterns, while others were expressed in all types of moss cells (Fig. 2E). We reasoned that stably expressed lncRNA-sORFs can produce peptides that play fundamental roles in various cellular processes. To explore this hypothesis, we examined the impact of lncRNA-sORF

Downloaded from genome.cshlp.org on June 13, 2026 . Published by Cold Spring Harbor Laboratory Press

overexpression and knockout on moss morphology using four lncRNAs-sORFs: Pp3c9_sORF1544, Pp3c25_sORF1253, Pp3c25_sORF1000 and Pp3c18_sORF57 (Fig. 2E). The translation of these SEPs was confirmed by several unique peptides and they contained "strong" and "medium" Kozak elements. We obtained multiple independent mutant lines for each of these lncRNAs-sORFs (Supplemental Figs. S9, S10, S11 and S12). Both the overexpression and knockout of sORFs resulted in morphological changes, implying that these peptides play a role in growth and development of *P. patens* (Figs. 4 and 5, Supplemental Table S6).

Overexpression of a 41-aa peptide (*PSEP1*, *Physcomitrella patens* sORF encoded peptide 1) encoded by the lncRNA-sORF Pp3c9_sORF1544 resulted in longer caulonema cells (filaments implicated in a rapid radial extension of the protonemal tissues) compared to the wild-type and *psep1* knockout lines (Fig. 4A-F and G, Supplemental Figs. S13A-F and S14A-D). Rapid growth in the *PSEP1* overexpressing lines (*OE*) was accompanied by earlier aging and cell death (Supplemental Fig. S15). By contrast, there was a small, but significant difference in growth rate between the wild-type and *psep1* mutant lines grown on solid media and in the liquid culture without glucose (Fig. 4H, Supplemental Fig. S13A-F).

The lines with a knockout in a 57-aa peptide (*psep3* KO) encoded by conservative lncRNA-sORF Pp3c25_sORF1253 displayed a decrease in growth rate and altered filament branching (Fig. 4I-O). In the wild-type moss plants, a pale-green diffuse network of caulonemal filaments surrounded the central zone (principally chloronemata), while *psep3* KO mutant lines displayed short lateral filaments on medium without glucose and ammonium tartrate, which favors chloronemal growth (Supplemental Fig. S13G-I). Overexpression of *PSEP3* (*PSEP3* OE) resulted in a significant decrease in growth rate compared to the wild type (Fig. 4P). Moreover, much of the *PSEP3* OE protonemal tissue grown on medium without ammonium tartrate turned brown (Fig. 5K-N, Supplemental Figure S14E-L).

Similar to the results for the *psep3* knockout, knocking out a 61-aa peptide (*psep25* KO) encoded by conserved lncRNA-sORF Pp3c25_sORF1000 also resulted in a decrease in growth rate and altered protonemal architecture on medium without glucose but supplemented with ammonium tartrate (Figs. 5A-G, Supplemental Fig. S13J-M). *PSEP25* - overexpressing mutant lines displayed a slight

Downloaded from genome.cshlp.org on June 13, 2026 . Published by Cold Spring Harbor Laboratory Press

decrease in growth rate compared to the wild-type (Fig. 5H) and almost no morphological differences in protonemal tissue structure (Supplemental Fig. S14M-P). In contrast to the *PSEP25* OE lines, *psep25* knockouts had a significant increase in the number of leafy shoots on medium without glucose but supplemented with ammonium tartrate, which usually reduces gametophore development (Figs. 5I-M). However, *PSEP25* OE mutant lines displayed an increase in the number of leafy shoots compared to the wild-type on solid medium without ammonium tartrate (Fig. 5K-N). Knocking out a 40-aa peptide (*psep18* KO) encoded by lncRNA-sORF Pp3c18_sORF57 showed a slight decrease in moss plant diameter on medium with glucose and without ammonium tartrate (Fig. 5O-Q; Supplemental Fig. S16A-C). However, only one *psep18* knockout line (Fig.5Q, KO-1) with deletion of a start codon had a significant decrease in growth rate compared to the wild-type. Taking into account that sORFs can trigger NMD in lncRNAs (Ruiz-Orera and Alba 2019), this fact requires more detailed investigation. *PSEP18* OE lines displayed a significant decrease in growth rate compared to the wild-type on medium with glucose (Fig. 5R-V; Supplemental Fig. S16D-F). We did not observe any changes in protonemal architecture and in the number of leafy shoots or filament branching in both overexpressing mutant lines and knockouts.

Taken together, our findings suggest that lncRNA-sORFs can influence growth and development in moss.

DISCUSSION

Although functionally characterized SEPs have been shown to play fundamental roles in key physiological processes, sORFs are arbitrarily excluded during genome annotation. Given the difficulty in identifying translatable, functional sORFs, we know little about their origin, evolution and regulation in the genome. In the present study, we investigated the abundance, evolutionary history and possible functions of sORFs in the genome of the model moss *Physcomitrella patens*. The use of an integrated pipeline that includes transcriptomics, proteomics, and peptidomics data allowed us to identify tens of small protein-coding sORFs in three types of moss cells.

Downloaded from genome.cshlp.org on June 13, 2026 . Published by Cold Spring Harbor Laboratory Press

sORFs with high coding potential are not conserved among genomes

Although analyzing the conservation of short amino acid sequences is not trivial (Moyers and Zhang 2016), hundreds of conserved sORFs have recently been identified in plants, yeast and animals (Ladoukakis et al. 2011; Hanada et al. 2013; Mackowiak et al. 2015; Brunet et al. 2019). The number of sORFs conserved in the plant kingdom is undoubtedly underestimated due to the low sensitivity of tools used for conservation analysis and the limited number of available sequenced genomes from closely related species. Our pipeline allowed us to identify 5034 conserved sORFs among the transcriptomes of ten different plant species, 5 of which showed evidence of translation according to our MS data. Three of five conserved sORFs belonged to lncRNAs. These data are in line with a previously published study showing that a large fraction of small ORFs in mouse genome evolves neutrally (Ruiz-Orera et al. 2018). We also found that uORFs and dORFs were significantly underrepresented among the sORFs that are conserved in the closest related species. We even detected rapid inactivation of uORFs and dORFs in the reconstructed genomes of three *P. patens* ecotypes due to disruptions in the start or stop codons (47% of the total disrupted sORFs). As the occurrence of sORFs downstream or upstream of the main ORF can be deleterious to its translation or induce nonsense-mediated decay (NMD), we cannot rule out the possibility that this may cause strong selection pressure and the rapid elimination of uORFs and dORFs (Iacono et al. 2005; Neafsey and Galagan 2007; Johnstone et al. 2016; Ruiz-Orera and Alba 2019). Taken together, these findings suggest that sORFs located in untranslated regions of mRNAs are evolving rapidly and may play regulatory roles rather than encoding bioactive peptides.

In recent studies, thousands of alternative proteins were experimentally detected in human cell lines (Vanderperre et al. 2013; Samandi et al. 2017; Brunet et al. 2019). In *P. patens*, we found tens of thousands of sORFs (CDS-sORFs) that overlapped with the CDS of protein-coding genes. The evolution of CDS-sORFs is undoubtedly an expensive process for the cell, as these elements may be located in regions encoding protein domains and influence the structure and function of the protein encoded by the main ORF (Cherry 2010). We found both CDS-sORFs originated from regions associated with known protein domains and CDS-sORFs from disordered regions, with higher conservation for CDS-sORFs originated from protein domain-encoding regions. These results

Downloaded from genome.cshlp.org on June 13, 2026 . Published by Cold Spring Harbor Laboratory Press

indicate that the evolution of CDS-sORFs depends on their locations insight main CDS sequence. However, whether sORFs are preferentially generated in fast-evolving regions of proteins or whether the selective pressure on sORFs leads to changes in protein-coding sequences is still unknown.

Analysis of sORF translation: approaches that makes sense

It was recently suggested that sORFs are randomly generated in a genome(Couso and Patraquim 2017). Assuming that the average length of a sORF is approximately 60 bp and that sORFs do not overlap, these elements occupy a substantial portion of the moss genome. This raises the question: to what extent are sORFs present in the transcriptome and the proteome of a cell? According to ribosome profiling data from a wide variety of species, sORFs translation appears to occur in a pervasive manner (Ingolia et al. 2011; Guttman et al. 2013; Bazzini et al. 2014; Couso and Patraquim 2017). However, ribosome-profiling data alone are not sufficient to classify transcripts as coding or noncoding (Guttman et al. 2013). Mass-spectrometry studies have thus far confirmed the presence of a few dozen SEPs in the peptidomes of animal cells (Slavoff et al. 2013; Prabakaran et al. 2014; Mackowiak et al. 2015; Ma et al. 2016; Tharakan et al. 2019). Comparisons of ribosome profiling and mass spectrometry results have led to the conclusion that MS detects peptides arising from the most highly translated sORFs (Aspden et al. 2014; Bazzini et al. 2014). However, a recent study showed that there are no technical obstacles to the detection of sORF-encoded peptides by mass spectrometry (Verheggen et al. 2017).

In previous studies, only standard proteomics analysis was used to identify SEPs. We reasoned that analyzing endogenous peptide pools instead of tryptic peptides has several disadvantages in terms of SEP identification: 1) standard proteomic approaches are not suitable for the isolation and analysis of small and low-abundance peptide molecules; and 2) SEPs are shorter than standard proteins and it is unlikely that more than one tryptic fragment will be detected in a single proteomic experiment. Moreover, peptidomic approaches can theoretically be used to identify full-length SEPs in a cell. We did not observe any significant overlap between the sORFs detected using proteomic and peptidomic approaches. Thus, our study demonstrates the advantage of using complementary approaches for building a complete list of SEPs.

Downloaded from genome.cshlp.org on June 13, 2026 . Published by Cold Spring Harbor Laboratory Press

382 According to our MS data, the translation patterns of most small protein-coding sORFs tend
383 to be tissue specific (Fig. 2A). We suggest that the slight overlap in tissue-specific expression among
384 SEPs from various types of moss cells could be due to either specific SEP post-translational
385 modification (PTM) patterns, tissue-specific transcription of sORFs, or the limitations of mass-
386 spectrometry in detecting low-abundance or modified sORF-encoded peptides. According to our
387 results, alternative splicing is an additional mechanism that control tissue-specific sORF expression
388 in plant cells. Also, the number of sORFs that were commonly translated between two types of moss
389 cells was higher for related cell types: protonemata and gametophores (two growth stages) as well
390 as protonemata and protoplasts (protoplasts were generated from the protonemata). These
391 observations indicate tissue-specific characteristics of SEPs translation and modification rather than
392 technical limitation in detection.

393 **Functionality of SEPs**

394 We identified tens of small protein-coding sORFs representing multiple sORF types and suggested
395 various functions for the types of sORFs. Clear evidence of transcription and translation points to a
396 possible biological significance of the small protein-coding sORFs that we identified here. Based on
397 our results (evolution, alternative splicing analysis), we suggest that the majority of uORFs play
398 regulatory roles instead of having peptide-encoding functions.
399 By contrast, CDS- and lncRNA-sORFs have greater potential to encode bioactive peptides, as they are
400 more highly conserved, frequently contain known protein domains and, according to the MS data,
401 produce peptides. We identified 19 small protein-coding CDS-sORFs in our dataset, seven of which
402 were translated simultaneously with previously annotated longer protein-coding ORF. This finding is
403 in agreement with a recent study on mammals, reporting that a gene MIEF1 translational product is
404 not the canonical protein but the small 70 amino acid alternative MiD51 protein is (Delcourt et al.
405 2018).

406 One possible role for CDS-sORFs that are similar to known proteins is to mimic the similar
407 protein to interfere with its function. MiPs (or siPEPs) are important modulators of protein–protein
408 and protein–DNA interactions that, for example, prevent the formation of functional protein
409 complexes (Seo et al. 2013; Graeff et al. 2016). We found that approximately 30% of cis-SEPs harbor

Downloaded from genome.cshlp.org on June 13, 2026 . Published by Cold Spring Harbor Laboratory Press

410 protein domains such as protein kinase domains and MYB-like DNA-binding domain or IDRs. Also,
411 some sORFs with disordered regions might mediate protein–protein or protein–nucleic acid
412 interactions, as suggested previously (Mackowiak et al. 2015). However, we failed to identify the
413 translation of such sORFs using stringent identification criteria in our mass-spectrometry analysis.
414 Therefore, this point requires further confirmation.

415 The transcription of the non-coding portions of the genome into lncRNAs is thought to give
416 rise to the translation of sORFs located within them. Nevertheless, the functions of these peptides are
417 unclear and require more detailed investigation. According to our results, knocking out the selected
418 lncRNA-encoded peptides was not lethal in moss, but did influenced moss growth and development.
419 All SEP knockouts showed a decrease in growth rate compared to the wild-type plants. By contrast,
420 we found that plants overexpressing lncRNA-encoded peptides showed more phenotypic differences
421 compared to the wild-type plants and knockouts. We observed both a significant increase in growth
422 rate (*PSEP1* OE) and in the number of leafy shoots (*PSEP25* OE) and a decrease in growth rate in
423 *PSEP3* OE, *PSEP18* OE, and *PSEP25* OE lines. The differences between the wild-type and mutant lines
424 often appeared only under certain growth conditions – solid or liquid media with/without glucose or
425 tartrate ammonia. These data may point to a tight regulation of lncRNA-encoded peptide translation
426 in cell. In light of these findings, we hypothesized that lncRNA-encoded peptides may not be vital but
427 be important for the survival under certain conditions by serving as a raw material for the evolution.
428 According to the recently proposed classification of small ORFs, lncRNA-sORFs used in our functional
429 analysis may be referred to both lncORFs and short CDSs (Couso and Patraquim 2017). Both short
430 CDSs and lncRNAs have a median size of 79 aa and 24 aa in animal genomes, respectively (Couso and
431 Patraquim 2017). We suggest that the differences in types of predicted sORFs between plant and
432 animal genomes require further investigation. Our results lay the groundwork for the systematic
433 analysis of functional peptides encoded by sORFs.

434 The possible evolution of non-coding portions of the genome into protein-coding genes is
435 also a subject of intensive debate (Carvunis et al. 2012; McLysaght and Guerzoni 2015; Couso and
436 Patraquim 2017; Ruiz-Orera and Alba 2019). According to our data, putative homologous sORFs
437 tended to differ in length in most cases. Thus, we suggest that most sORFs expanded during

Downloaded from genome.cshlp.org on June 13, 2026 . Published by Cold Spring Harbor Laboratory Press

evolution, providing support for the notion that they function as raw materials for selection; however, this point requires further confirmation.

METHODS

Physcomitrella patens growth conditions

Physcomitrella patens subsp. *patens* ("Gransden 2004", Frieburg) protonemata were grown on BCD medium supplemented with 5 mM ammonium tartrate (BCDAT) or 0.5% glucose during a 16-h photoperiod at 25^{0}C in 9-cm Petri dishes (Nishiyama et al. 2000). For all analyses, the protonemata were collected every 5 days. The gametophores were grown on free-ammonium tartrate BCD medium under the same conditions, and 8-week-old gametophores were used for analysis. Protoplast was prepared from protonemata as described previously (Fesenko et al. 2015).

For morphological analysis, protonemal tissue 2 mm in diameter were inoculated on BCD and BCDAT 9-cm Petri dishes. For growth rate measurements, photographs were taken at 7 d intervals over 42 days. Protonemal tissues and cells were photographed using a Microscope Digital Eyepiece DCM-510 attached to a Stemi 305 stereomicroscope or Olympus CKX41.

Identification of coding sORFs in the *P. patens* genome

To identify sORFs with high coding potential, the sORFfinder (Hanada et al. 2010) tool was utilized. Intron sequences and CDS were used as negative and positive sets, respectively. Additional details are described in the Supplemental Methods. To select for sORFs that are transcribed, located in the exons of transcripts, and have introns, a BED file was generated using a Python script (GffParser.py) and intersected with exon positions extracted from a gff3 file of *P. patens* genome annotations. To identify intergenic-sORFs, the BED file was also intersected with transcribed regions determined based on our RNA-seq data (Fesenko et al. 2017). Using an R script, sORFs fully overlapping with exons were removed; 75,685 sORFs remained after this step. Identical sORFs were removed from the dataset. In addition, sORFs overlapping repetitive regions identified by RepeatMasker (Tempel 2012), as well as sORFs comprising parts of annotated *P. patens* main and alternative protein

Downloaded from genome.cshlp.org on June 13, 2026 . Published by Cold Spring Harbor Laboratory Press

isoforms, were also removed from the dataset, resulting in a final dataset of sORFs comprising 70,095 sequences.

sORF classification

The step-by-step procedure performed for sORF classification is illustrated in Supplemental Fig. S17. In the first step, lncRNA-sORFs were identified by searching for identical sORFs in known lncRNA databases, including CANTATAdb (Szczesniak et al. 2016), GreeNC (Paytuvi Gallart et al. 2016) and our previously published moss dataset (Fesenko et al. 2017). After this sORF BED file was intersected with the latest moss genome annotation V3.3 (Lang et al. 2018). The locations of the sORFs on transcripts were determined, resulting in the further classification of genic-sORFs into uORFs, dORFs, CDS-sORFs and interlaced-sORFs. sORFs were denoted as upstream or downstream if they were fully separated from the longer protein-coding ORF as previously described (Calviello et al. 2016; Samandi et al. 2017).

Because alternative splicing leads to inaccuracy in genome annotation, the locations of a subset of genic-sORFs cannot be unambiguously classified, as they can be located in different regions in different isoforms of the same gene. All sORFs located on transcripts that were not annotated in the *P. patens* genome V3.3 but were identified using our RNA-seq data were classified as intergenic-sORFs. To detect alternatively spliced sORFs (AS-sORFs), a BED file with sORF locations was intersected with a BED file containing intron coordinates for all isoforms. Those sORFs that overlapped for both exons (see above) and introns were classified as AS-sORFs.

Evolutionary conservation analysis

The transcriptomes of nine plant species were downloaded from Phytozome v12: *Sphagnum fallax* (release 0.5), *Marchantia polymorpha* (release 3.1), *Selaginella moellendorffii* (release 1.0), *Spirodela polyrhiza* (release 2), *Arabidopsis thaliana* (TAIR 10), *Zea mays* (Ensembl-18), *Oryza sativa* (release 7), *Volvox carteri* (release 2.1) and *Chlamydomonas reinhardtii* (release 5.5). The transcriptome of *Ceratodon purpureus* was *de novo* assembled using Trinity (Haas et al. (2013)). To identify

Downloaded from genome.cshlp.org on June 13, 2026 . Published by Cold Spring Harbor Laboratory Press

transcribed homologous sequences, TBLASTN (word size = 3) was performed using sORF peptide sequences as queries and the transcriptome sequences of the abovementioned species as subjects. The following cutoffs parameters were used to distinguish reliable alignments: e-value < 10^{-6} and query coverage > 60%. Our e-value cutoff was obtained by applying a multiple comparison correction (Bonferroni correction) of 0.05, which is commonly used in biological experiments.

Pairwise K_A/K_S ratios were calculated using the codeml algorithm with PAML software (Yang 2007). The calculation procedure, which was facilitated using a custom-made Python script (protein_Ka_Ks_codeml.py), included alignment extraction from the TBLASTN output, PAL2NAL (Suyama et al. 2006) correction of the nucleotide alignment using the corresponding aligned protein sequences and calculation of K_A/K_S ratios using codeml. The script implements packages from biopython (Cock et al. 2009). To estimate homologous sORF lengths, a Python script (sORF_completeness_v2.0.py) was designed. Additional details are described in the Supplemental Methods.

Gene Ontology (GO) terms enrichment analysis

GO enrichment analysis was performed using the topGO bioconductor R package using the Fisher's exact test in conjunction with the 'classic' algorithm (false discovery rate [FDR] < 0.05). GO terms assigned to *P. patens* genes were downloaded from Phytozome. Only GO terms containing >5 genes in a background dataset were considered in the enrichment analysis. Redundant GO terms were removed using the web-based tool REVIGO (Supek et al. 2011).

Peptide and protein extraction

Endogenous peptide extraction was conducted as described previously (Fesenko et al. 2015). Proteins were extracted as described previously (Fesenko et al. 2016). Additional details are described in the Supplemental Methods.

Mass-spectrometry analysis and peptide identification

Mass-spectrometry analysis was performed using three biological and three technical repeats for the proteomic and peptidomic datasets (Supplementary Table S2). Analysis was performed on two

Downloaded from genome.cshlp.org on June 13, 2026 . Published by Cold Spring Harbor Laboratory Press

different mass spectrometers: a TripleTOF 5600+ mass spectrometer with a NanoSpray III ion source (ABSciex,Canada) and a Q Exactive HF mass spectrometer (Q Exactive HF Hybrid Quadrupole-Orbitrap mass spectrometer, Thermo Fisher Scientific, USA). Additional details are described in the Supplemental Methods.

All datasets were searched individually with MaxQuant v1.5.8.3 (Tyanova et al. 2016) against a custom database containing 32926 proteins from annotated genes in the latest version of the moss genome (V3.3, (Lang et al. 2018)), 85 moss chloroplast proteins, 42 moss mitochondrial proteins and 70052 predicted sORF peptides (Supplemental Code). MaxQuant's protein FDR filter was disabled, while 1% FDR was used to select high-confidence PSMs, and ambiguous peptides were filtered out. Moreover, any PSMs with Andromeda scores of less than 30 were discarded (to exclude poor MS/MS spectra). For the dataset of endogenous peptides (named "peptidomic", Supplementary Table S2), the parameter "Digestion Mode" was set to "unspecific" and modifications were not permitted. All other parameters were left as default values. For the dataset of tryptic peptides (named "proteomic") the parameter "Digestion Mode" was set to "specific" (the Trypsin/P), MaxQuant's protein FDR filter was disabled, and the peptide FDR remained at 1%. All other parameters were left as default values. Features of the PSMs (length, intensity, number of spectra, Andromeda score, intensity coverage and peak coverage) were extracted from MaxQuant's msms.txt files. Annotated spectra for identified sORFs were exported from MaxQuant (Supplemental Fig. S18) and manually inspected.

To filter out MS peptides that do not provide unambiguous evidence of sORF peptide expression, we assessed the number of times a peptide occurred in the whole moss genome by searching for exact matches to the MS peptides in the six-frame translated genome (see Supplemental Methods).

RT-PCR analysis of AS-sORFs

Total RNA from gametophores, protonema and protoplasts was isolated as previously described (Cove et al. 2009). RNA quality and quantity were evaluated via electrophoresis in an agarose gel with ethidium bromide staining. The precise concentration of total RNA in each sample was measured using a Quant-iT™ RNA Assay Kit, 5–100 ng on a Qubit 3.0 (Invitrogen, US) fluorometer. The cDNA for RT-PCR was synthesized using an MMLV RT Kit (Evrogen, Russia) according to the

Downloaded from genome.cshlp.org on June 13, 2026 . Published by Cold Spring Harbor Laboratory Press

manufacturer's recommendations employing oligo(dT)17 -primers from 2 µg total RNA after DNase treatment. The primers were designed using Primer-BLAST (Ye et al. 2012) (Supplemental Table S7). The minus reverse transcriptase control (-RT) contained RNA without reverse transcriptase treatment to confirm the absence of DNA in the samples. The RT-PCR products were resolved on an 1.5% agarose gel and visualized using ethidium bromide staining.

Generation of overexpression and knockout lines

To obtain PSEP1 (Pp3c9_sORF1544), PSEP3 (Pp3c25_sORF1253), PSEP25 (Pp3c25_sORF1000) and PSPE18 (Pp3c18_sORF57) overexpression lines, PCR was carried out using genomic DNA as a template and the PEP4f, PEP4r, pep3FXho, pep3RNhe, pep25FXho, pep25RNhe, pep18FXho and pep18RNhe primers, respectively (Supplemental Table S7). Amplicons were cloned into the pPLV27 vector (GenBank JF909480) using the ligation-independent cloning (LIC) procedure (Aslanidis and de Jong 1990; De Rybel et al. 2011). The resulting plasmids were named pPLV-Hpa-4FR (*PSEP1*), pPLV-Hpa-3FR (*PSEP3*), pPLV-Hpa-25FR (*PSEP25*), pPLV-Hpa-18FR (*PSEP18*) and used for transformation. Additional details are described in the Supplemental Methods.

PSEP1 (sORF Pp3c9_sORF1544), PSEP3 (Pp3c25_sORF1253), PSEP25 (Pp3c25_sORF1000), PSPE18 (sORF Pp3c18_sORF57) knockout lines were created using the CRISPR/Cas9 system (Collonnier et al. 2017). The coding sequences were used to search for CRISPR RNA (crRNA) preceded by a *S. pyogenes* Cas9 PAM motif (NGG) using the web tool CRISPR DESIGN (http://crispr.mit.edu/). The crRNA closest to the translation start site (ATG) was selected for cloning (Supplemental Table S7).

Protoplasts were transformed using PEG transformation protocol (Schaefer and Zryd 1997). Additional details are described in the Supplemental Methods. The plasmids pACT-CAS9 (for CAS9 expression) and pBNRF (resistance to G418) were kindly provided by Dr. Fabien Nogué. Independent knockout and overexpression mutant lines have been obtained (Supplemental Figs. S9-12).

The ploidy level of the *PSEP1* overexpression and *psep1* knock-out lines were estimated using flow cytometry. Protoplasts were fixed in cold 70% methanol, washed in TBS with 0.1% Triton X-100, then washed with TBS and stained with 500 ng/ml DAPI. The fluorescence was analyzed with a

Downloaded from genome.cshlp.org on June 13, 2026 . Published by Cold Spring Harbor Laboratory Press

574 flow cytometer NovoCyte (ACEA Biosciences) and Novoexpress data software. Fluorescence was
575 excited at 405 nm, and detection was at 445/45 nm.
576
577 **DATA ACCESS**
578 All raw mass spectrometry data from this study have been deposited to the ProteomeXchange
579 Consortium via the PRIDE (Vizcaino et al. 2016) partner repository with the dataset identifiers
580 PXD007922, PXD007923, PXD007973.
581
582 **SOFTWARE AVAILABILITY**
583 All data were analyzed using Python (http://www.python.org, v 3.5), and R (R Core Team 2017). All
584 scripts are available at Zenodo (doi: 10.5281/zenodo.1160331) and are maintained in the GitHub
585 code repository: https://github.com/Kirovez/Scripts_sORFs_MS and in Supplemental Code.
586
587 **ACKNOWLEDGEMENTS**
588 We thank Dr. James Lloyd for his assistance in NMD-targeted transcript analysis. This work was supported
589 by the Russian Science Foundation (project No.17-14-01189). Some of mass spectrometric
590 measurements were performed using the equipment of the “Human Proteome” Core Facility of the
591 Orekhovich Institute of Biomedical Chemistry (Russia) which is supported by the Ministry of
592 Education and Science of the Russian Federation.
593 **Authors’ contributions**
594 IF and IK conceived and designed experiments. AK, AM performed moss transformation experiments.
595 RK, VL, DK, EG, VZ, IB and AM performed the proteomics analyses. IF, IK and GA performed the
596 statistical and bioinformatics analyses. IF, IK, VI and VG wrote the manuscript with input from all
597 authors. IF supervised the project. All authors read and approved the final manuscript.
598 **DISCLOSURE DECLARATION**
599 The authors declare that they have no significant competing financial, professional, or personal
600 interests that might have influenced the performance or presentation of the work described in this
601 manuscript.

Downloaded from genome.cshlp.org on June 13, 2026 . Published by Cold Spring Harbor Laboratory Press

602

603 **REFERENCES**

604 Andrews SJ, Rothnagel JA. 2014. Emerging evidence for functional peptides encoded by short
605 open reading frames. *Nat Rev Genet* **15**(3): 193-204.
606 Aslanidis C, de Jong PJ. 1990. Ligation-independent cloning of PCR products (LIC-PCR).
607 *Nucleic acids research* **18**(20): 6069-6074.
608 Aspden JL, Eyre-Walker YC, Phillips RJ, Amin U, Mumtaz MA, Brocard M, Couso JP. 2014.
609 Extensive translation of small Open Reading Frames revealed by Poly-Ribo-Seq. *eLife*
610 **3**: e03528.
611 Barbosa C, Peixeiro I, Romao L. 2013. Gene expression regulation by upstream open reading
612 frames and human disease. *PLoS genetics* **9**(8): e1003529.
613 Bazzini AA, Johnstone TG, Christiano R, Mackowiak SD, Obermayer B, Fleming ES, Vejnar CE,
614 Lee MT, Rajewsky N, Walther TC et al. 2014. Identification of small ORFs in
615 vertebrates using ribosome footprinting and evolutionary conservation. *The EMBO*
616 *journal* **33**(9): 981-993.
617 Blanvillain R, Young B, Cai YM, Hecht V, Varoquaux F, Delorme V, Lancelin JM, Delseny M,
618 Gallois P. 2011. The Arabidopsis peptide kiss of death is an inducer of programmed
619 cell death. *The EMBO journal* **30**(6): 1173-1183.
620 Brunet MA, Brunelle M, Lucier JF, Delcourt V, Levesque M, Grenier F, Samandi S, Leblanc S,
621 Aguilar JD, Dufour P et al. 2019. OpenProt: a more comprehensive guide to explore
622 eukaryotic coding potential and proteomes. *Nucleic acids research* **47**(D1): D403-
623 D410.
624 Calviello L, Mukherjee N, Wyler E, Zauber H, Hirsekorn A, Selbach M, Landthaler M,
625 Obermayer B, Ohler U. 2016. Detecting actively translated open reading frames in
626 ribosome profiling data. *Nature methods* **13**(2): 165-170.
627 Carvunis AR, Rolland T, Wapinski I, Calderwood MA, Yildirim MA, Simonis N, Charloteaux B,
628 Hidalgo CA, Barbette J, Santhanam B et al. 2012. Proto-genes and de novo gene birth.
629 *Nature* **487**(7407): 370-374.
630 Chang CY, Lin WD, Tu SL. 2014. Genome-Wide Analysis of Heat-Sensitive Alternative Splicing
631 in Physcomitrella patens. *Plant Physiol* **165**(2): 826-840.
632 Cherry JL. 2010. Expression level, evolutionary rate, and the cost of expression. *Genome*
633 *biology and evolution* **2**: 757-769.
634 Chilley PM, Casson SA, Tarkowski P, Hawkins N, Wang KL, Hussey PJ, Beale M, Ecker JR,
635 Sandberg GK, Lindsey K. 2006. The POLARIS peptide of Arabidopsis regulates auxin
636 transport and root growth via effects on ethylene signaling. *Plant Cell* **18**(11): 3058-
637 3072.
638 Cock PJ, Antao T, Chang JT, Chapman BA, Cox CJ, Dalke A, Friedberg I, Hamelryck T, Kauff F,
639 Wilczynski B et al. 2009. Biopython: freely available Python tools for computational
640 molecular biology and bioinformatics. *Bioinformatics* **25**(11): 1422-1423.
641 Collonnier C, Epert A, Mara K, Maclot F, Guyon-Debast A, Charlot F, White C, Schaefer DG,
642 Nogue F. 2017. CRISPR-Cas9-mediated efficient directed mutagenesis and RAD51-
643 dependent and RAD51-independent gene targeting in the moss Physcomitrella
644 patens. *Plant Biotechnol J* **15**(1): 122-131.
645 Couso JP. 2015. Finding smORFs: getting closer. *Genome Biol* **16**: 189.
646 Couso JP, Patraquim P. 2017. Classification and function of small open reading frames.
647 *Nature reviews Molecular cell biology* **18**(9): 575-589.
648 Cove DJ, Perroud PF, Charron AJ, McDaniel SF, Khandelwal A, Quatrano RS. 2009. Isolation of
649 DNA, RNA, and protein from the moss Physcomitrella patens gametophytes. *Cold*
650 *Spring Harbor protocols* **2009**(2): pdb prot5146.

Downloaded from genome.cshlp.org on June 13, 2026 . Published by Cold Spring Harbor Laboratory Press

D'Lima NG, Ma J, Winkler L, Chu Q, Loh KH, Corpuz EO, Budnik BA, Lykke-Andersen J, Saghatelian A, Slavoff SA. 2017. A human microprotein that interacts with the mRNA decapping complex. *Nat Chem Biol* **13**(2): 174-180.

De Coninck B, Carron D, Tavormina P, Willem L, Craik DJ, Vos C, Thevissen K, Mathys J, Cammue BP. 2013. Mining the genome of Arabidopsis thaliana as a basis for the identification of novel bioactive peptides involved in oxidative stress tolerance. *J Exp Bot* **64**(17): 5297-5307.

De Rybel B, van den Berg W, Lokerse A, Liao CY, van Mourik H, Moller B, Peris CL, Weijers D. 2011. A versatile set of ligation-independent cloning vectors for functional studies in plants. *Plant Physiol* **156**(3): 1292-1299.

Delcourt V, Brunelle M, Roy AV, Jacques JF, Salzet M, Fournier I, Roucou X. 2018. The Protein Coded by a Short Open Reading Frame, Not by the Annotated Coding Sequence, Is the Main Gene Product of the Dual-Coding Gene MIEF1. *Mol Cell Proteomics* **17**(12): 2402-2411.

Djordjevic MA, Mohd-Radzman NA, Imin N. 2015. Small-peptide signals that control root nodule number, development, and symbiosis. *J Exp Bot* **66**(17): 5171-5181.

Eguen T, Straub D, Graeff M, Wenkel S. 2015. MicroProteins: small size-big impact. *Trends Plant Sci* **20**(8): 477-482.

Fesenko I, Khazigaleeva R, Kirov I, Kniazev A, Glushenko O, Babalyan K, Arapidi G, Shashkova T, Butenko I, Zgoda V et al. 2017. Alternative splicing shapes transcriptome but not proteome diversity in Physcomitrella patens. *Scientific reports* **7**(1): 2698.

Fesenko I, Seredina A, Arapidi G, Ptushenko V, Urban A, Butenko I, Kovalchuk S, Babalyan K, Knyazev A, Khazigaleeva R et al. 2016. The Physcomitrella patens Chloroplast Proteome Changes in Response to Protoplastation. *Front Plant Sci* **7**: 1661.

Fesenko IA, Arapidi GP, Skripnikov AY, Alexeev DG, Kostryukova ES, Manolov AI, Altukhov IA, Khazigaleeva RA, Seredina AV, Kovalchuk SI et al. 2015. Specific pools of endogenous peptides are present in gametophore, protonema, and protoplast cells of the moss Physcomitrella patens. *Bmc Plant Biol* **15**: 87.

Ge Y, Porse BT. 2014. The functional consequences of intron retention: alternative splicing coupled to NMD as a regulator of gene expression. *BioEssays : news and reviews in molecular, cellular and developmental biology* **36**(3): 236-243.

Giannakakis A, Zhang J, Jenjaroenpun P, Nama S, Zainolabidin N, Aau MY, Yarmishyn AA, Vaz C, Ivshina AV, Grinchuk OV et al. 2015. Contrasting expression patterns of coding and noncoding parts of the human genome upon oxidative stress. *Scientific reports* **5**: 9737.

Graeff M, Straub D, Eguen T, Dolde U, Rodrigues V, Brandt R, Wenkel S. 2016. MicroProtein-Mediated Recruitment of CONSTANS into a TOPLESS Trimeric Complex Represses Flowering in Arabidopsis. *PLoS genetics* **12**(3): e1005959.

Guillen G, Diaz-Camino C, Loyola-Torres CA, Aparicio-Fabre R, Hernandez-Lopez A, Diaz-Sanchez M, Sanchez F. 2013. Detailed analysis of putative genes encoding small proteins in legume genomes. *Front Plant Sci* **4**.

Guttman M, Russell P, Ingolia NT, Weissman JS, Lander ES. 2013. Ribosome Profiling Provides Evidence that Large Noncoding RNAs Do Not Encode Proteins. *Cell* **154**(1): 240-251.

Hanada K, Akiyama K, Sakurai T, Toyoda T, Shinozaki K, Shiu SH. 2010. sORF finder: a program package to identify small open reading frames with high coding potential. *Bioinformatics* **26**(3): 399-400.

Hanada K, Higuchi-Takeuchi M, Okamoto M, Yoshizumi T, Shimizu M, Nakaminami K, Nishi R, Ohashi C, Iida K, Tanaka M et al. 2013. Small open reading frames associated with morphogenesis are hidden in plant genomes. *P Natl Acad Sci USA* **110**(6): 2395-2400.

Downloaded from genome.cshlp.org on June 13, 2026 . Published by Cold Spring Harbor Laboratory Press

Hanada K, Zhang X, Borevitz JO, Li WH, Shiu SH. 2007. A large number of novel coding small open reading frames in the intergenic regions of the Arabidopsis thaliana genome are transcribed and/or under purifying selection. *Genome Res* **17**(5): 632-640.

Hellens RP, Brown CM, Chisnal MAW, Waterhouse PM, Macknight RC. 2016. The Emerging World of Small ORFs. *Trends Plant Sci* **21**(4): 317-328.

Huang JZ, Chen M, Chen, Gao XC, Zhu S, Huang H, Hu M, Zhu H, Yan GR. 2017. A Peptide Encoded by a Putative lncRNA HOXB-AS3 Suppresses Colon Cancer Growth. *Mol Cell* **68**(1): 171-184 e176.

Iacono M, Mignone F, Pesole G. 2005. uAUG and uORFs in human and rodent 5'untranslated mRNAs. *Gene* **349**: 97-105.

Ingolia NT, Lareau LF, Weissman JS. 2011. Ribosome Profiling of Mouse Embryonic Stem Cells Reveals the Complexity and Dynamics of Mammalian Proteomes. *Cell* **147**(4): 789-802.

Johnstone TG, Bazzini AA, Giraldez AJ. 2016. Upstream ORFs are prevalent translational repressors in vertebrates. *The EMBO journal* **35**(7): 706-723.

Karousis ED, Nasif S, Muhlemann O. 2016. Nonsense-mediated mRNA decay: novel mechanistic insights and biological impact. *Wiley interdisciplinary reviews RNA* **7**(5): 661-682.

Kastenmayer JP, Ni L, Chu A, Kitchen LE, Au WC, Yang H, Carter CD, Wheeler D, Davis RW, Boeke JD et al. 2006. Functional genomics of genes with small open reading frames (sORFs) in S-cerevisiae. *Genome Res* **16**(3): 365-373.

Kim TS, Liu CL, Yassour M, Holik J, Friedman N, Buratowski S, Rando OJ. 2010. RNA polymerase mapping during stress responses reveals widespread nonproductive transcription in yeast. *Genome Biol* **11**(7): R75.

Kondo T, Plaza S, Zanet J, Benrabah E, Valenti P, Hashimoto Y, Kobayashi S, Payre F, Kageyama Y. 2010. Small Peptides Switch the Transcriptional Activity of Shavenbaby During Drosophila Embryogenesis. *Science* **329**(5989): 336-339.

Kozak M. 1986. Point mutations define a sequence flanking the AUG initiator codon that modulates translation by eukaryotic ribosomes. *Cell* **44**(2): 283-292.

-. 1997. Recognition of AUG and alternative initiator codons is augmented by G in position +4 but is not generally affected by the nucleotides in positions +5 and +6. *The EMBO journal* **16**(9): 2482-2492.

Ladoukakis E, Pereira V, Magny EG, Eyre-Walker A, Couso JP. 2011. Hundreds of putatively functional small open reading frames in Drosophila. *Genome Biol* **12**(11).

Laing WA, Martinez-Sanchez M, Wright MA, Bulley SM, Brewster D, Dare AP, Rassam M, Wang D, Storey R, Macknight RC et al. 2015. An Upstream Open Reading Frame Is Essential for Feedback Regulation of Ascorbate Biosynthesis in Arabidopsis. *Plant Cell* **27**(3): 772-786.

Lang D, Ullrich KK, Murat F, Fuchs J, Jenkins J, Haas FB, Piednoel M, Gundlach H, Van Bel M, Meyberg R et al. 2018. The Physcomitrella patens chromosome-scale assembly reveals moss genome structure and evolution. *Plant J* **93**(3): 515-533.

Lauressergues D, Couzigou JM, Clemente HS, Martinez Y, Dunand C, Becard G, Combier JP. 2015. Primary transcripts of microRNAs encode regulatory peptides. *Nature* **520**(7545): 90-93.

Lease KA, Walker JC. 2006. The Arabidopsis unannotated secreted peptide database, a resource for plant peptidomics. *Plant Physiol* **142**(3): 831-838.

Lloyd JPB, Lang D, Zimmer AD, Causier B, Reski R, Davies B. 2018. The loss of SMG1 causes defects in quality control pathways in Physcomitrella patens. *Nucleic acids research* **46**(11): 5822-5836.

Downloaded from genome.cshlp.org on June 13, 2026 . Published by Cold Spring Harbor Laboratory Press

Ma J, Diedrich JK, Jungreis I, Donaldson C, Vaughan J, Kellis M, Yates JR, 3rd, Saghatelian A. 2016. Improved Identification and Analysis of Small Open Reading Frame Encoded Polypeptides. *Analytical chemistry* **88**(7): 3967-3975.

Mackowiak SD, Zauber H, Bielow C, Thiel D, Kutz K, Calviello L, Mastrobuoni G, Rajewsky N, Kempa S, Selbach M et al. 2015. Extensive identification and analysis of conserved small ORFs in animals. *Genome Biol* **16**.

Magny EG, Pueyo JI, Pearl FM, Cespedes MA, Niven JE, Bishop SA, Couso JP. 2013. Conserved regulation of cardiac calcium uptake by peptides encoded in small open reading frames. *Science* **341**(6150): 1116-1120.

Matsumoto A, Pasut A, Matsumoto M, Yamashita R, Fung J, Monteleone E, Saghatelian A, Nakayama KI, Clohessy JG, Pandolfi PP. 2017. mTORC1 and muscle regeneration are regulated by the LINC00961-encoded SPAR polypeptide. *Nature* **541**(7636): 228-232.

Mazin PV, Fisunov GY, Gorbachev AY, Kapitskaya KY, Altukhov IA, Semashko TA, Alexeev DG, Govorun VM. 2014. Transcriptome analysis reveals novel regulatory mechanisms in a genome-reduced bacterium. *Nucleic acids research* **42**(21): 13254-13268.

McLysaght A, Guerzoni D. 2015. New genes from non-coding sequence: the role of de novo protein-coding genes in eukaryotic evolutionary innovation. *Philosophical transactions of the Royal Society of London Series B, Biological sciences* **370**(1678): 20140332.

Moyers BA, Zhang J. 2016. Evaluating Phylostratigraphic Evidence for Widespread De Novo Gene Birth in Genome Evolution. *Molecular biology and evolution* **33**(5): 1245-1256.

Narita NN, Moore S, Horiguchi G, Kubo M, Demura T, Fukuda H, Goodrich J, Tsukaya H. 2004. Overexpression of a novel small peptide ROTUNDIFOLIA4 decreases cell proliferation and alters leaf shape in Arabidopsis thaliana. *Plant J* **38**(4): 699-713.

Neafsey DE, Galagan JE. 2007. Dual modes of natural selection on upstream open reading frames. *Molecular biology and evolution* **24**(8): 1744-1751.

Nelson BR, Makarewich CA, Anderson DM, Winders BR, Troupes CD, Wu F, Reese AL, McAnally JR, Chen X, Kavalali ET et al. 2016. A peptide encoded by a transcript annotated as long noncoding RNA enhances SERCA activity in muscle. *Science* **351**(6270): 271-275.

Nishiyama T, Hiwatashi Y, Sakakibara I, Kato M, Hasebe M. 2000. Tagged mutagenesis and gene-trap in the moss, Physcomitrella patens by shuttle mutagenesis. *DNA research : an international journal for rapid publication of reports on genes and genomes* **7**(1): 9-17.

Paytuvi Gallart A, Hermoso Pulido A, Anzar Martinez de Lagran I, Sanseverino W, Aiese Cigliano R. 2016. GREENC: a Wiki-based database of plant lncRNAs. *Nucleic acids research* **44**(D1): D1161-1166.

Popp MW, Maquat LE. 2013. Organizing principles of mammalian nonsense-mediated mRNA decay. *Annual review of genetics* **47**: 139-165.

Prabakaran S, Hemberg M, Chauhan R, Winter D, Tweedie-Cullen RY, Dittrich C, Hong E, Gunawardena J, Steen H, Kreiman G et al. 2014. Quantitative profiling of peptides from RNAs classified as noncoding. *Nature communications* **5**: 5429.

R Core Team. 2017. R: A Language and Environment for Statistical Computing.

Rasheed S, Bashir K, Nakaminami K, Hanada K, Matsui A, Seki M. 2016. Drought stress differentially regulates the expression of small open reading frames (sORFs) in Arabidopsis roots and shoots. *Plant signaling & behavior* **11**(8): e1215792.

Rensing SA, Ick J, Fawcett JA, Lang D, Zimmer A, Van de Peer Y, Reski R. 2007. An ancient genome duplication contributed to the abundance of metabolic genes in the moss Physcomitrella patens. *BMC evolutionary biology* **7**: 130.

Downloaded from genome.cshlp.org on June 13, 2026 . Published by Cold Spring Harbor Laboratory Press

Rensing SA, Lang D, Zimmer AD, Terry A, Salamov A, Shapiro H, Nishiyama T, Perroud PF, Lindquist EA, Kamisugi Y et al. 2008. The Physcomitrella genome reveals evolutionary insights into the conquest of land by plants. *Science* **319**(5859): 64-69.

Rohrig H, Schmidt J, Miklashevichs E, Schell J, John M. 2002. Soybean ENOD40 encodes two peptides that bind to sucrose synthase. *Proc Natl Acad Sci U S A* **99**(4): 1915-1920.

Rothnagel J, Menschaert G. 2018. Short Open Reading Frames and Their Encoded Peptides. *Proteomics* **18**(10): e1700035.

Rubtsova M, Naraykina Y, Vasilkova D, Meerson M, Zvereva M, Prassolov V, Lazarev V, Manuvera V, Kovalchuk S, Anikanov N et al. 2018. Protein encoded in human telomerase RNA is involved in cell protective pathways. *Nucleic acids research* **46**(17): 8966-8977.

Ruiz-Orera J, Alba MM. 2019. Translation of Small Open Reading Frames: Roles in Regulation and Evolutionary Innovation. *Trends in genetics : TIG* **35**(3): 186-198.

Ruiz-Orera J, Verdaguer-Grau P, Villanueva-Canas JL, Messeguer X, Alba MM. 2018. Translation of neutrally evolving peptides provides a basis for de novo gene evolution. *Nature ecology & evolution* **2**(5): 890-896.

Samandi S, Roy AV, Delcourt V, Lucier JF, Gagnon J, Beaudoin MC, Vanderperre B, Breton MA, Motard J, Jacques JF et al. 2017. Deep transcriptome annotation enables the discovery and functional characterization of cryptic small proteins. *eLife* **6**.

Schaefer DG, Zryd JP. 1997. Efficient gene targeting in the moss Physcomitrella patens. *Plant J* **11**(6): 1195-1206.

Seo PJ, Hong SY, Kim SG, Park CM. 2011. Competitive inhibition of transcription factors by small interfering peptides. *Trends Plant Sci* **16**(10): 541-549.

Seo PJ, Park MJ, Park CM. 2013. Alternative splicing of transcription factors in plant responses to low temperature stress: mechanisms and functions. *Planta* **237**(6): 1415-1424.

Slavoff SA, Mitchell AJ, Schwaid AG, Cabili MN, Ma J, Levin JZ, Karger AD, Budnik BA, Rinn JL, Saghatelian A. 2013. Peptidomic discovery of short open reading frame-encoded peptides in human cells. *Nat Chem Biol* **9**(1): 59-+.

Staudt AC, Wenkel S. 2011. Regulation of protein function by 'microProteins'. *EMBO reports* **12**(1): 35-42.

Supek F, Bosnjak M, Skunca N, Smuc T. 2011. REVIGO summarizes and visualizes long lists of gene ontology terms. *Plos One* **6**(7): e21800.

Suyama M, Torrents D, Bork P. 2006. PAL2NAL: robust conversion of protein sequence alignments into the corresponding codon alignments. *Nucleic acids research* **34**(Web Server issue): W609-612.

Szczesniak MW, Rosikiewicz W, Makalowska I. 2016. CANTATAdb: A Collection of Plant Long Non-Coding RNAs. *Plant Cell Physiol* **57**(1): e8.

Tavormina P, De Coninck B, Nikonorova N, De Smet I, Cammue BP. 2015. The Plant Peptidome: An Expanding Repertoire of Structural Features and Biological Functions. *Plant Cell* **27**(8): 2095-2118.

Tempel S. 2012. Using and understanding RepeatMasker. *Methods Mol Biol* **859**: 29-51.

Tharakan R, Kreimer S, Ubaida-Mohien C, Lavoie J, Olexiouk V, Menschaert G, Ingolia NT, Cole RN, Ishizuka K, Sawa A et al. 2019. A methodology for discovering novel brain-relevant peptides: Combination of ribosome profiling and peptidomics. *Neuroscience research*.

Tyanova S, Temu T, Cox J. 2016. The MaxQuant computational platform for mass spectrometry-based shotgun proteomics. *Nat Protoc* **11**(12): 2301-2319.

van der Lee R, Buljan M, Lang B, Weatheritt RJ, Daughdrill GW, Dunker AK, Fuxreiter M, Gough J, Gsponer J, Jones DT et al. 2014. Classification of intrinsically disordered regions and proteins. *Chemical reviews* **114**(13): 6589-6631.

Downloaded from genome.cshlp.org on June 13, 2026 . Published by Cold Spring Harbor Laboratory Press

Vanderperre B, Lucier JF, Bissonnette C, Motard J, Tremblay G, Vanderperre S, Wisztorski M, Salzet M, Boisvert FM, Roucou X. 2013. Direct Detection of Alternative Open Reading Frames Translation Products in Human Significantly Expands the Proteome. *Plos One* **8**(8).

Verheggen K, Volders PJ, Mestdagh P, Menschaert G, Van Damme P, Gevaert K, Martens L, Vandesompele J. 2017. Noncoding after All: Biases in Proteomics Data Do Not Explain Observed Absence of lncRNA Translation Products. *J Proteome Res* **16**(7): 2508-2515.

Vizcaino JA, Csordas A, Del-Toro N, Dianes JA, Griss J, Lavidas I, Mayer G, Perez-Riverol Y, Reisinger F, Ternent T et al. 2016. 2016 update of the PRIDE database and its related tools. *Nucleic acids research* **44**(22): 11033.

Wu HP, Su YS, Chen HC, Chen YR, Wu CC, Lin WD, Tu SL. 2014. Genome-wide analysis of light-regulated alternative splicing mediated by photoreceptors in Physcomitrella patens. *Genome Biol* **15**(1): R10.

Yang Z. 2007. PAML 4: phylogenetic analysis by maximum likelihood. *Molecular biology and evolution* **24**(8): 1586-1591.

Ye J, Coulouris G, Zaretskaya I, Cutcutache I, Rozen S, Madden TL. 2012. Primer-BLAST: a tool to design target-specific primers for polymerase chain reaction. *Bmc Bioinformatics* **13**: 134.

FIGURE LEGENDS

Fig. 1. Several distinct types of sORFs are present in the moss genome. A – Pipeline used in this study to identify coding sORFs; **B** – Proposed classification of sORFs according to the types of encoding transcripts: upstream ORFs (uORFs) and downstream ORFs (dORFs) in the untranslated regions (UTRs) of canonical mRNAs; CDS-sORFs, which overlap with protein-coding sequences in alternative (+2 or +3) reading frames or are truncated versions of proteins generated by alternative splicing; interlaced-sORFs, which overlap both the protein-coding sequence and UTR on the same transcript; lncRNA-sORFs and intergenic sORFs, which are located on short non-protein coding transcripts.; **C** – Boxplot of the length distribution of sORFs in different groups.

Fig. 2. Moss contains tens of small protein-coding sORFs. A – Venn diagram showing the distribution of the identified translatable sORFs among three types of moss cells; **B** – Length distribution of various groups of small protein-coding sORFs; **C** - Distribution of small protein-coding sORFs based on the suggested classification; **D** – Binary heatmap showing evidence of translation for sORFs and proteins in multicoding genes in three moss tissues. G, N and P correspond to gametophores, protonemata and protoplasts, respectively; **E** – Heatmap showing expression levels (log10 (RPKM)) for the lncRNAs (left) carrying sORFs (lncRNA-sORFs) and binary heatmap showing

Downloaded from genome.cshlp.org on June 13, 2026 . Published by Cold Spring Harbor Laboratory Press

887 evidence of translation (determined as whether a peptide was identified (brown) or not (grey) in MS
888 data) for the corresponding lncRNA-sORFs (right) in three moss tissues, gametophores (G),
889 protonemata (N) and protoplasts (P).

890 **Fig. 3. Venn diagram showing the number of AS-sORFs influenced by different AS events.**

891 **Fig. 4. Morphology of wild type and sORF-encoded peptide mutant lines. The phenotypes of**
892 ***psep1* KO and *PSEP1* OE lines grown on BCD medium with 0.5% glucose:** A, D – wild type; B, E -
893 knockout of *PSEP1*; C, F – overexpression of *PSEP1*; G - the diameter of moss plants with
894 overexpression of *PSEP1* (Supplemental Figure S14A-D, Supplemental Table S6); H - the diameter of
895 moss plants with knockout of *PSEP1* (Supplemental Figure S13A-C, Supplemental Table S6). **The**
896 **phenotypes of *psep3* KO and *PSEP3* OE lines grown on BCD medium:** I, L **-** wild type; J, M -
897 knockout of *PSEP3*; K, N - overexpression of *PSEP3*; O - the diameter of moss plants with knockout of
898 *PSEP3* (Supplemental Figure S13G-I, Supplemental Table S6); P - the diameter of moss plants with
899 overexpression of the *PSEP3* (Supplemental Figure S14E-H, Supplemental Table S6). Scale bar: 0.5
900 mm. *P*-value was calculated by Student's unpaired *t*-test. ****P-value < 0.0001; ***P-value < 0.001
901 **P-value < 0.01; *P-value < 0.05.

902 **Fig. 5. Morphology of wild type and sORF-encoded peptide mutant lines. The phenotypes of**
903 ***psep25* KO and *PSEP25* OE lines grown on BCDAT medium:** A, D - wild type; B, E - knockout of
904 *PSEP25*; C, F – overexpression of *PSEP25*; G - the diameter of moss plants with knockout of PSEP25
905 (Supplemental Figure S13J-M, Supplemental Table S6); H - the diameter of moss plants with
906 overexpression of PSEP25 (Supplemental Figure S14M-P, Supplemental Table S6); I, J, M - the
907 number of leafy shoots in wild type and three *psep25* KO lines. K, L, N - the number of leafy shoots in
908 wild type and two *PSEP25* OE lines on BCD medium. Arrows show young leafy gametophores. **The**
909 **phenotypes of psep18 KO and PSEP18 OE lines grown on BCD medium with 0.5% glucose:** O, R,
910 T – wild type; P - knockout of *PSEP18*; Q - the diameter of moss plants with knockout of *PSEP18*
911 (Supplemental Figure S16A-C, Supplemental Table S6); S, U– overexpression of *PSEP18*; V - the
912 diameter of moss plants with overexpression of *PSEP18* (Supplemental Figure S16D-F, Supplemental
913 Table S6).

Downloaded from genome.cshlp.org on June 13, 2026 . Published by Cold Spring Harbor Laboratory Press

914 Scale bar: 0.5 mm. *P*-value was calculated by Student's unpaired *t*-test. ****P-value < 0.0001; ***P-

915 value < 0.001 **P-value < 0.01; *P-value < 0.05.

A

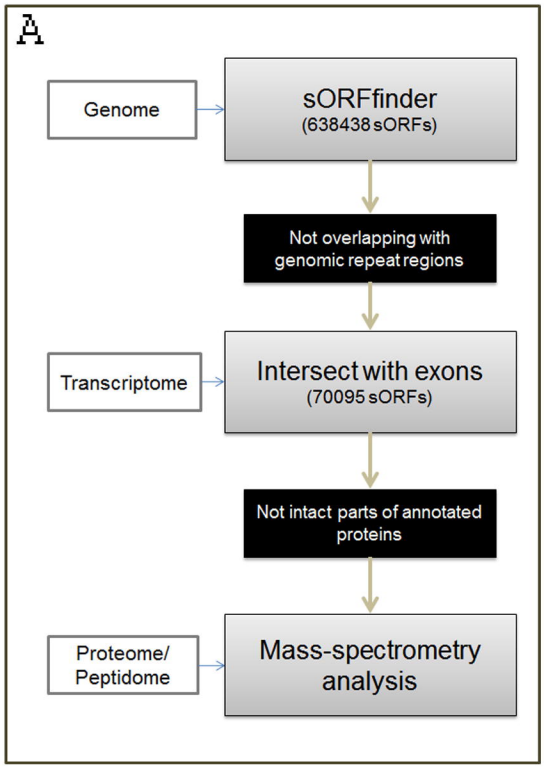

C

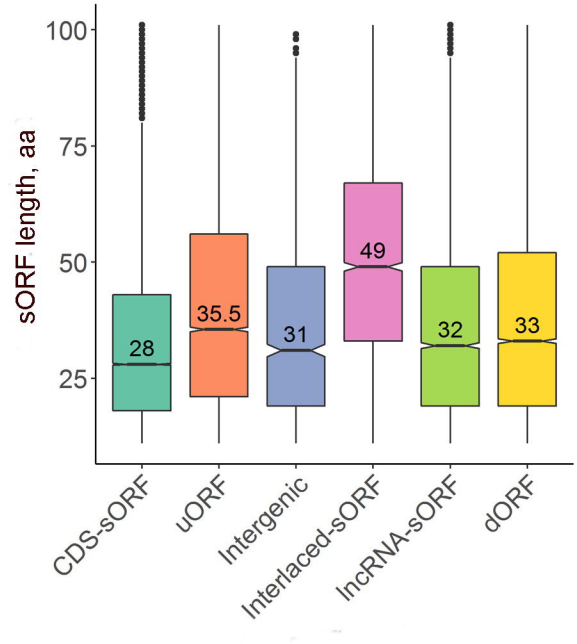

B

sORF class	RNA type	Evidence of transcription (RNA-seq data)	Evidence of translation (MS data)
Upstream sORFs (uORFs)	5'-AAAA-3'	11998	6
Downstream sORFs (dORFs)	5'-AAAA-3'	9444	9
Coding sequence-sORFs (CDS-sORFs)	5'-AAAA-3'	36732	19
Interlaced-sORFs	5'-AAAA-3'	3485	2
Intergenic/ lncRNA-sORFs	5'-AAAA-3'	1241/5745	1/9

main ORF | untranslated region | sORF | intron

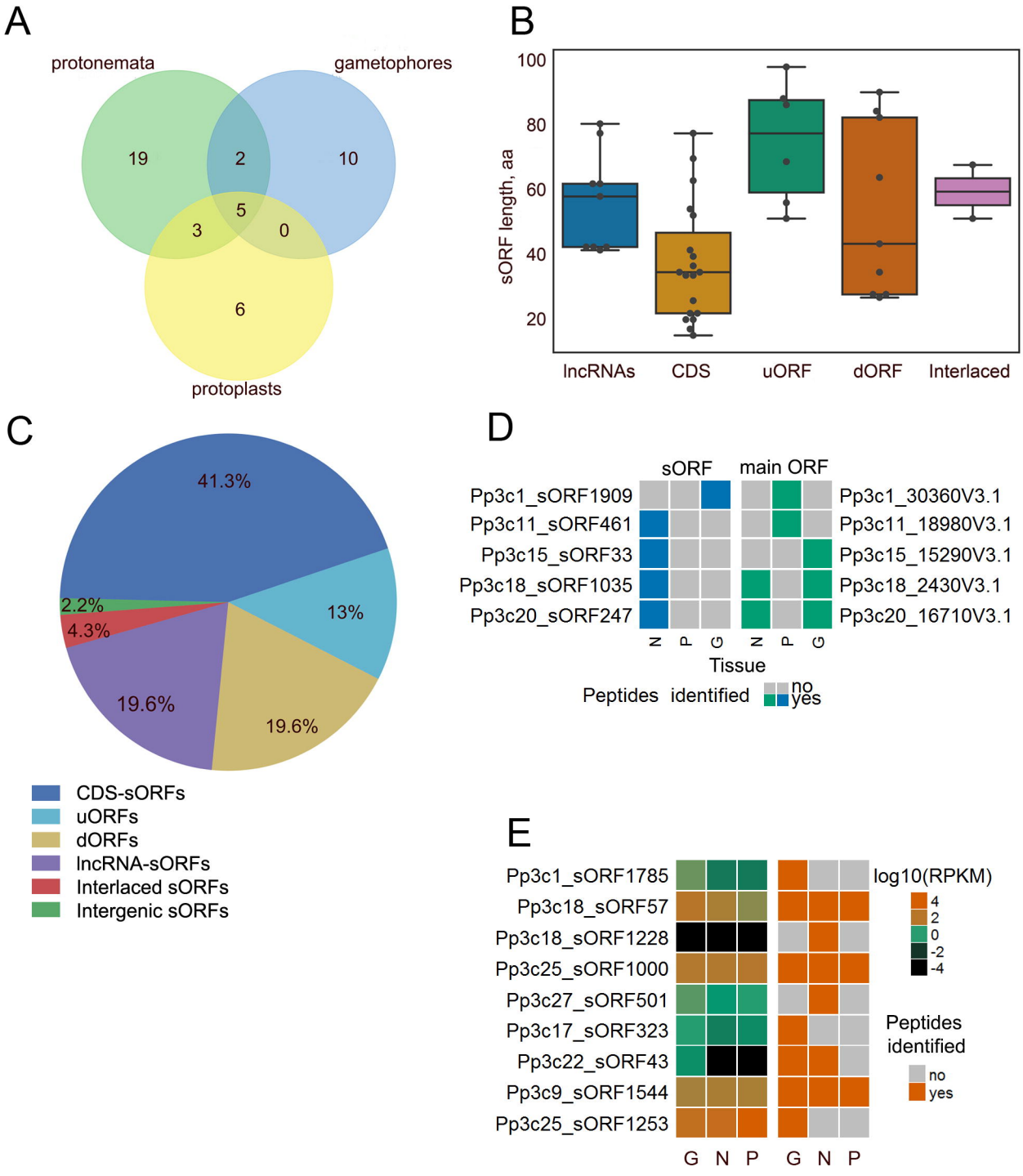
A
protonemata
gametophores
protoplasts
19
2
10
5
3
0
6
B
sORF length, aa
100
80
60
40
20
lncRNAs
CDS
uORF
dORF
Interlaced
C
41.3%
13%
19.6%
19.6%
4.3%
2.2%
CDS-sORFs
uORFs
dORFs
lncRNA-sORFs
Interlaced sORFs
Intergenic sORFs
D
sORF
main ORF
Pp3c1_sORF1909
Pp3c11_sORF461
Pp3c15_sORF33
Pp3c18_sORF1035
Pp3c20_sORF247
Pp3c1_30360V3.1
Pp3c11_18980V3.1
Pp3c15_15290V3.1
Pp3c18_2430V3.1
Pp3c20_16710V3.1
N
P
G
Tissue
Peptides identified
no
yes
E
Pp3c1_sORF1785
Pp3c18_sORF57
Pp3c18_sORF1228
Pp3c25_sORF1000
Pp3c27_sORF501
Pp3c17_sORF323
Pp3c22_sORF43
Pp3c9_sORF1544
Pp3c25_sORF1253
G N P G N P
log10(RPKM)
4
2
0
-2
-4
Peptides identified
no
yes

Downloaded from genome.cshlp.org on June 13, 2026 . Published by Cold Spring Harbor Laboratory Press

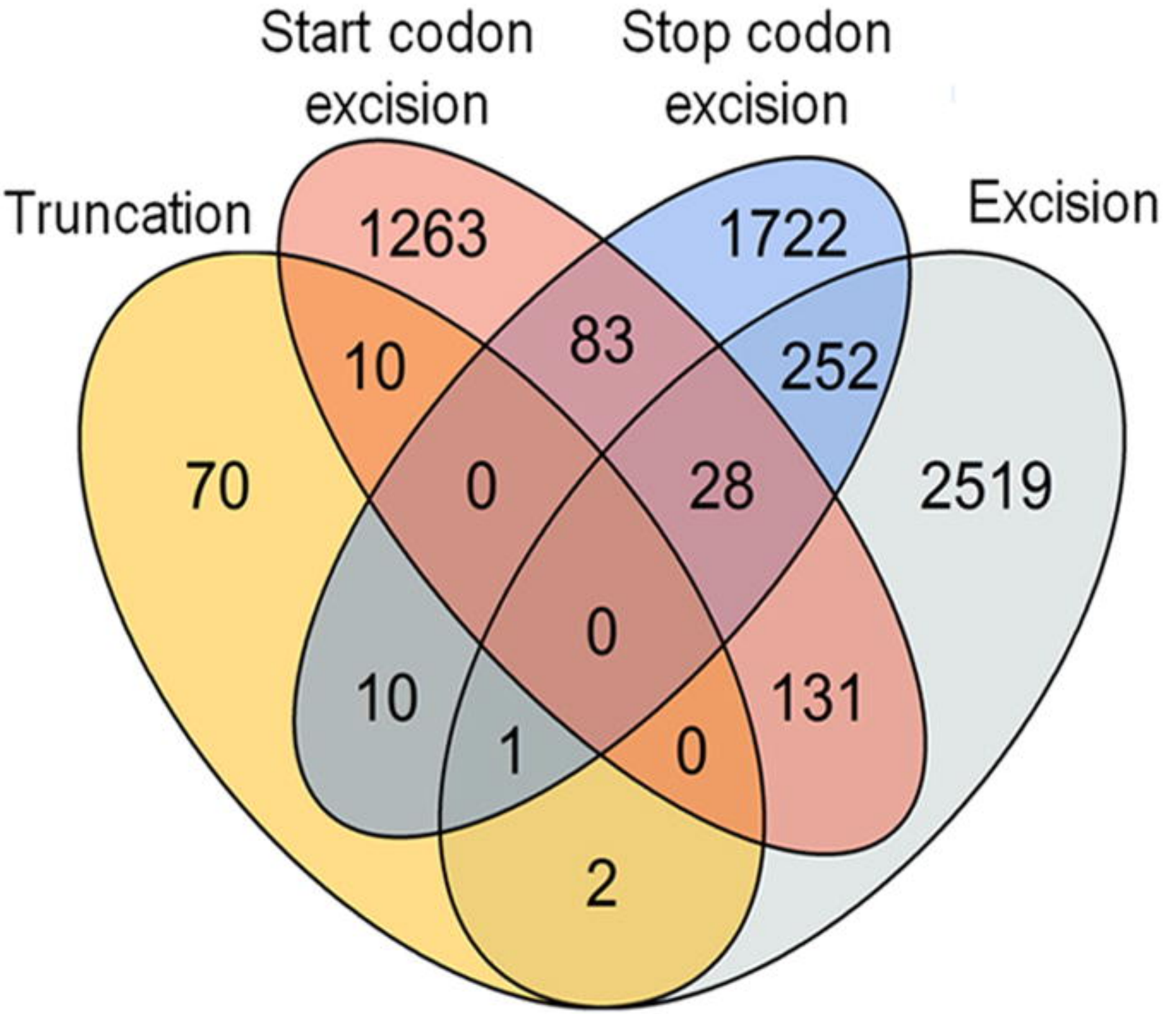

A peptide PSEP1

MVQPLLARLASAAEFVALPGAILVAYFSTSRSTEPKRDHRK (41 aa)

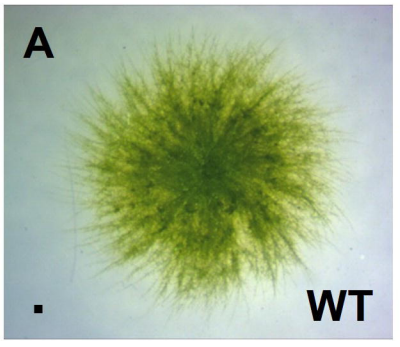

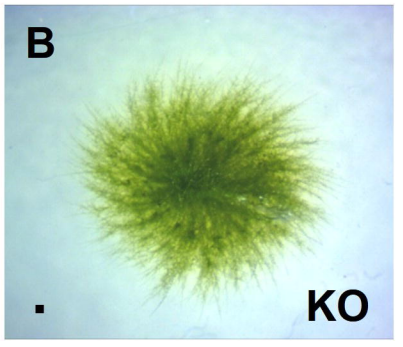

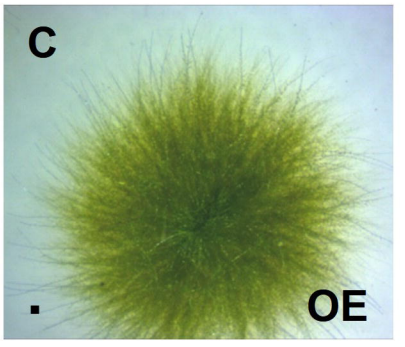

Downloaded from genome.cshlp.org on June 13, 2026 . Published by Cold Spring Harbor Laboratory Press

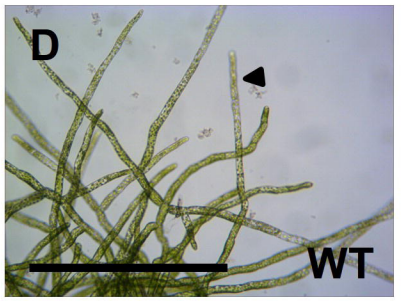

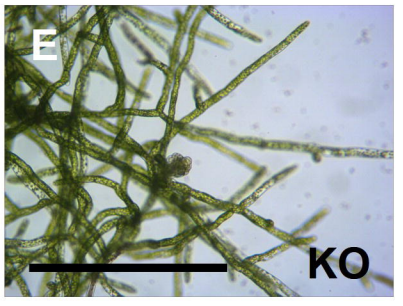

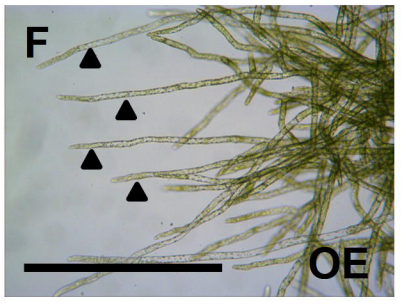

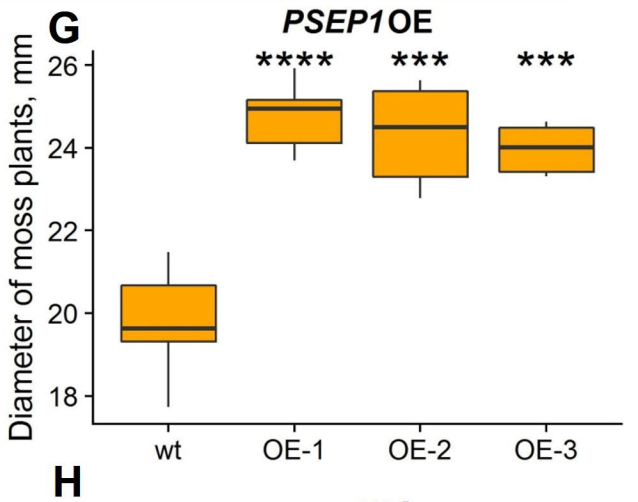

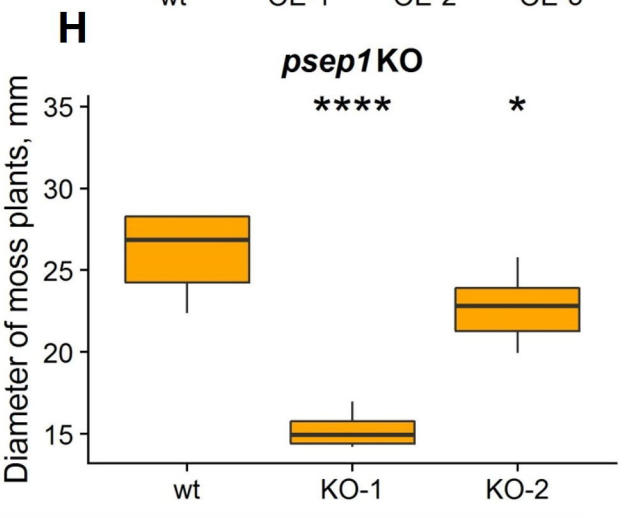

A peptide PSEP3

MVHQDNSGSGLRSFNHPNPPPNNNRPPSNPPVVRNPSSGRTPHPYPPPPHNYNGYPN (57 aa)

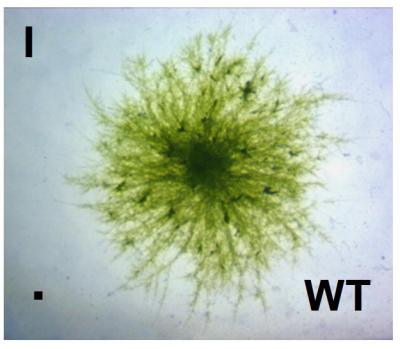

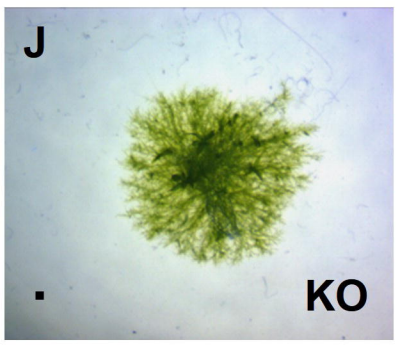

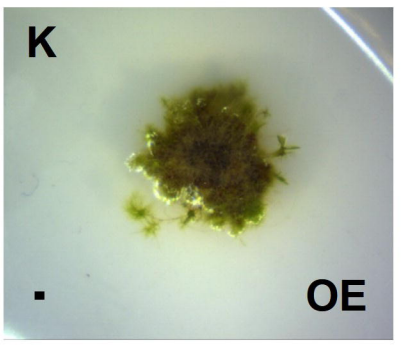

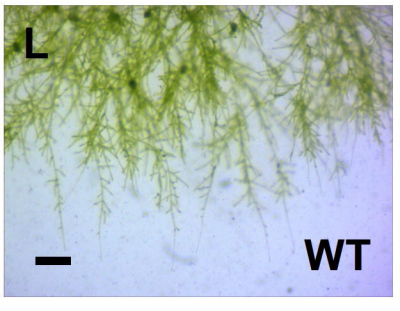

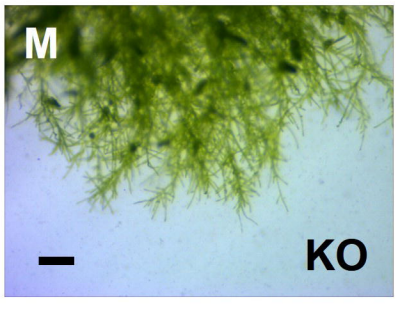

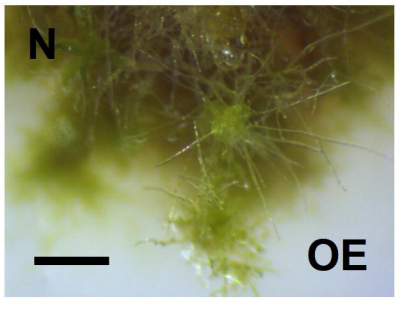

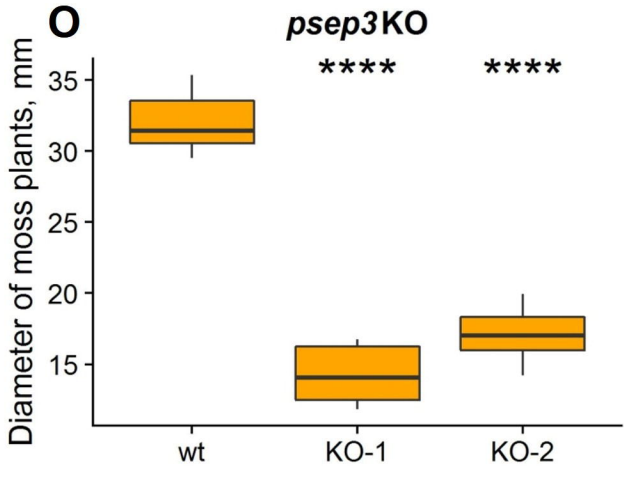

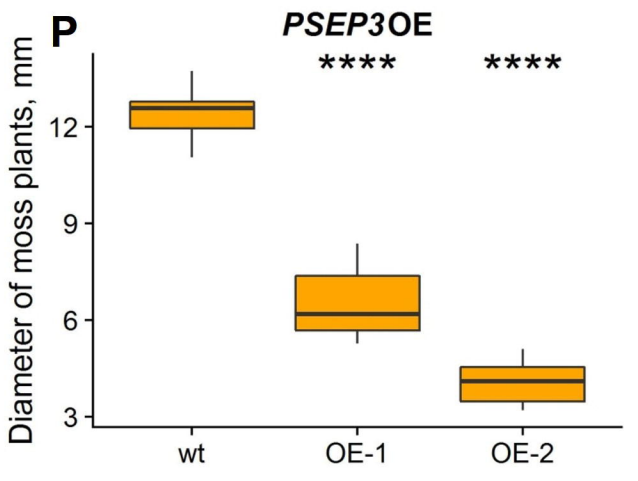

A peptide PSEP25

MVQSKQGLSLLKFIPKVIRPQTSDVSSAVLWGTTAACGALWLVQPFDWIKEQITGPKEESK (61 aa)

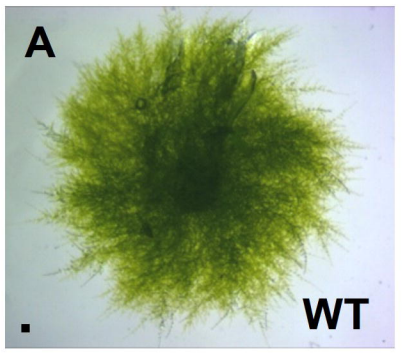

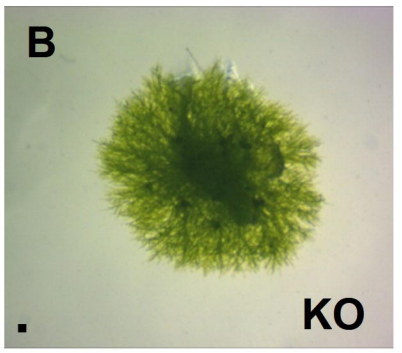

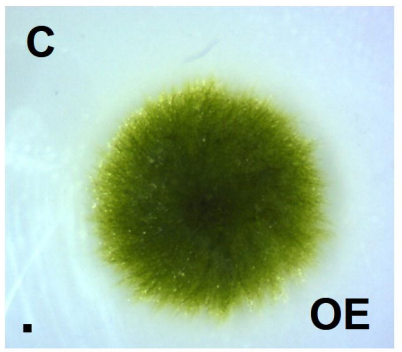

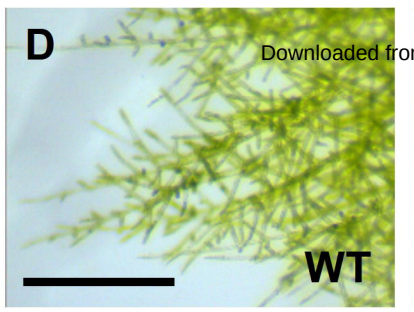

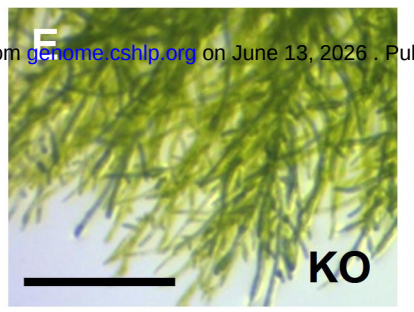

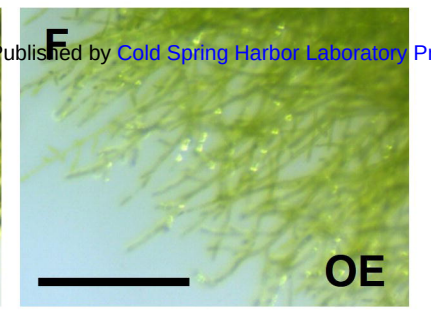

Downloaded from genome.cshlp.org on June 13, 2026 . Published by Cold Spring Harbor Laboratory Press

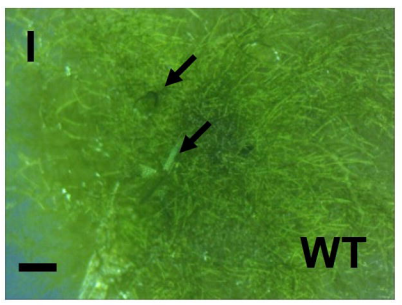

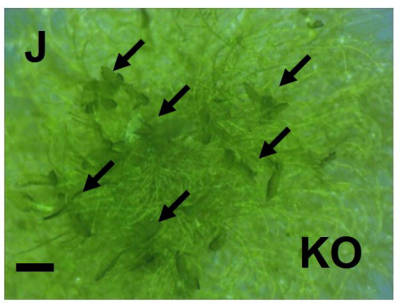

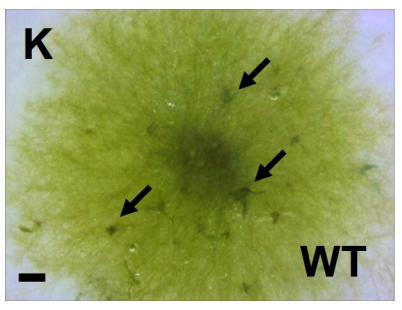

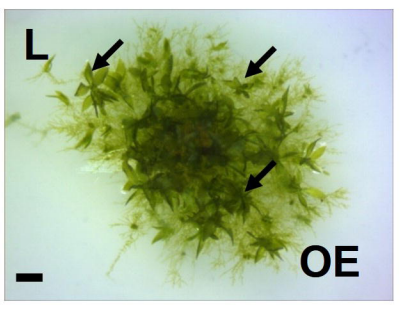

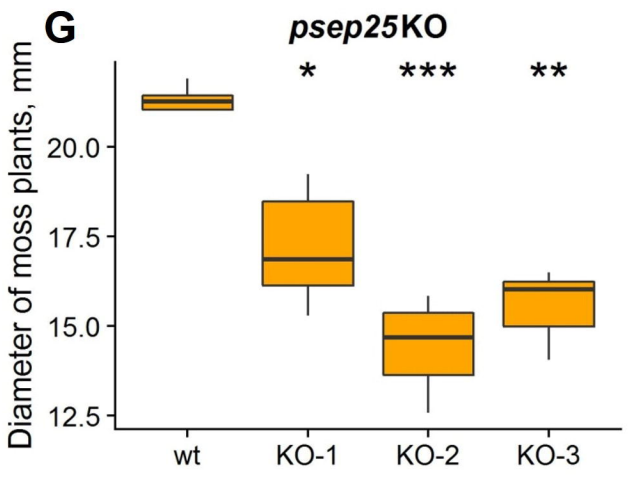

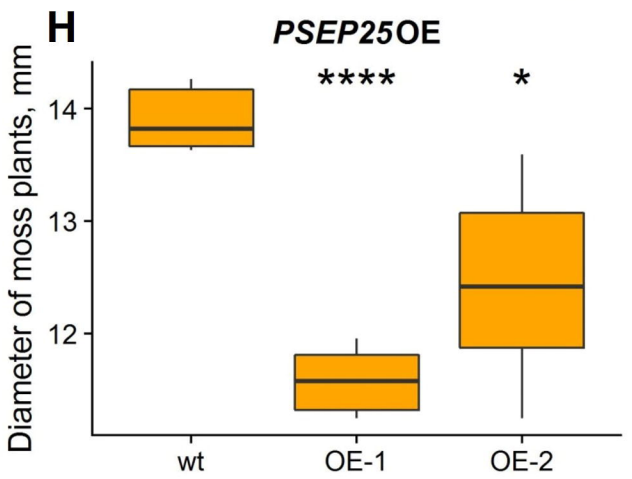

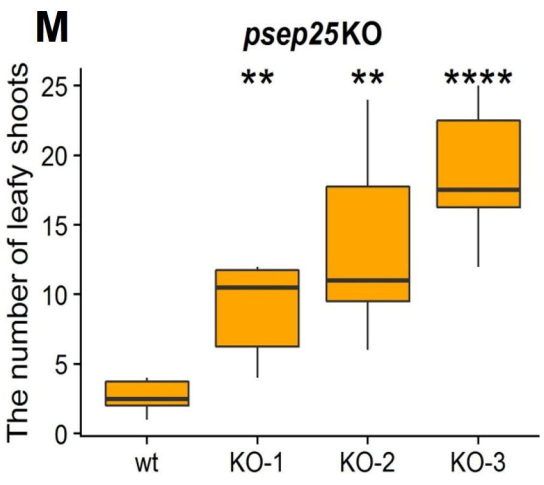

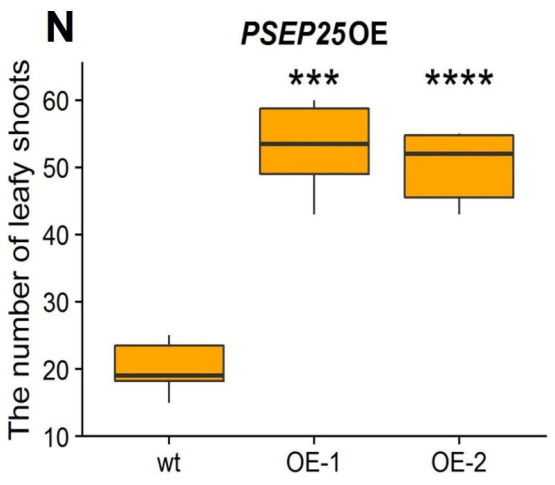

A peptide PSEP18

MQAFTDTQGYSSFNGPATTAATTPPEVVGEFGGKGWRPSS (40 aa)